Coreopsis tinctoria

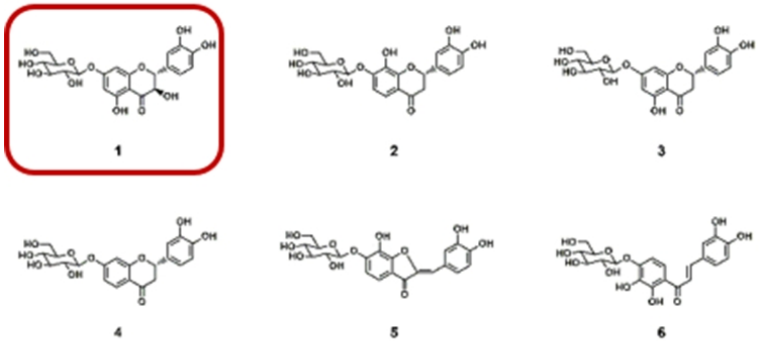

Anti-oxidant

Nrf2↑

HO-1 ↑

SOD ↑
GPx ↑

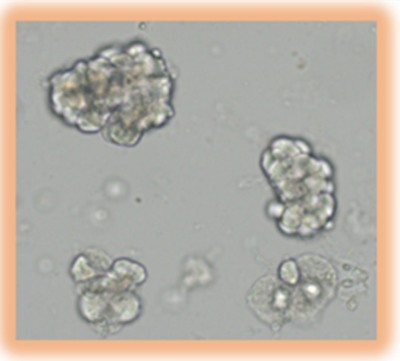

Acinar cells necrosis ↓
ROS production ↓

Three independent experimental acute pancreatitis models↓

Research Article

Protective effects of flavonoids from *Coreopsis tinctoria* Nutt. on experimental acute pancreatitis via Nrf-2/ARE-mediated antioxidant pathways

Dan Du [a,1,*], Linbo Yao [b,1], Rui Zhang [c], Na Shi [b], Yan Shen [c], Xinmin Yang [b], Xiaoying Zhang [b], Tao Jin [b], Tingting Liu [b], Liqiang Hu [a], Zhihua Xing [c], David N Criddle [d], Qing Xia [b], Wei Huang [b,e,*], Robert Sutton [e]

[a] West China-Washington Mitochondria and Metabolism Centre, West China Hospital, Sichuan University, Chengdu 610041, China; [b] Department of Integrated Traditional Chinese and Western Medicine, Sichuan Provincial Pancreatitis Centre and West China-Liverpool Biomedical Research Centre, West China Hospital, Sichuan University, Chengdu 610041, China; [c] Laboratory of Ethnopharmacology, West China Hospital, Sichuan University, Chengdu 610041, China; [d] Department of Cellular and Molecular Physiology, Institute of Translational Medicine, University of Liverpool, Liverpool L69 3BX, UK; [e] Liverpool Pancreatitis Study Group, Institute of Translational Medicine, University of Liverpool, Liverpool L69 3GE, UK

[1] These authors contributed equally to this work.

Correspondence to: Wei Huang, Department of Integrated Traditional Chinese and Western Medicine, 10th Floor 3rd Inpatient Building, West China Hospital of Sichuan University, No. 37 Wannan Guoxue Road, Chengdu 610041, Sichuan Province, China. E-mail: dr_wei_huang@163.com; Dan Du, West China-Washington Mitochondria and Metabolism Centre, 5A Floor 2nd Building, Tianfu Life Science Park of Hi-Tech Industrial Development Zone, No. 88 Keyuan South Road, Chengdu 610041, Sichuan Province, China. E-mail: dudan1520@163.com

Abstract

Ethnopharmacological relevance: Oxidative stress is a prominent feature of clinical acute pancreatitis (AP). *Coreopsis tinctoria* has been used traditionally to treat pancreas disorders like diabetes mellitus in China and Portugal and its flavonoid-rich fraction contain the main phytochemicals that have antioxidant and anti-inflammatory activities.

Aim of the study: To investigate the effects of flavonoids isolated from *C. tinctoria* on experimental AP and explore the potential mechanism.

Material and methods: LC-MS based online technique was used to analyse and isolate targeted flavonoids from *C. tinctoria*. Freshly isolated mouse pancreatic acinar cells were treated with taurocholic acid sodium salt hydrate (NaT, 5 mM) with or without flavonoids. Fluorescence microscopy and a plate reader were used to determine necrotic cell death pathway activation (propidium iodide), reactive oxygen species (ROS) production (H2-DCFDA) and ATP depletion (luminescence) where appropriate. AP was induced by 7 repeated intraperitoneal caerulein injections (50 μg/kg) at hourly interval in mice or retrograde infusion of taurolithocholic acid 3-sulfate disodium salt (TLCS; 5 mM, 50 μL) into the pancreatic duct in mice or infusion of NaT (3.5%, 1 mL/kg) in rats. A flavonoid was intraperitoneally administered at 0, 4, and 8 hours after the first caerulein injection or post-operation. Disease severity, oxidative stress and antioxidant markers were determined.

Results: Total flavonoids extract and flavonoids 1-6 (C**1**-C**6**) exhibited different capacities in reducing necrotic cell death pathway activation with 0.5 mM C**1**, (2R,3R)-taxifolin 7-O-*β*-D-glucopyranoside, having the best effect. C**1** also significantly reduced NaT-induced ROS production and ATP depletion. C**1** at 12.5 mg/kg and 8.7 mg/kg (equivalent to 12.5 mg/kg for mice) significantly reduced histopathological, biochemical and immunological parameters in the caerulein-, TLCS- and NaT-induced AP models, respectively. C**1** administration increased pancreatic nuclear factor erythroid 2-related factor 2 (Nrf2) and Nrf2-medicated haeme oxygenase-1 expression and elevated pancreatic antioxidant enzymes superoxide dismutase and glutathione peroxidase levels.

Conclusions: Flavonoid C**1** from *C. tinctoria* was protective in experimental AP and this effect may at least in part be attributed to its antioxidant effects by activation of Nrf2-mediated pathways. These results suggest the potential utilisation of *C. tinctoria* to treat AP.

Keywords: *Coreopsis tinctoria*; flavonoids; acute pancreatitis; oxidative stress; Nrf2; antioxidant enzymes.

Abbreviations: AP, acute pancreatitis; AREs, antioxidant response elements; BCA, bicinchoninic acid protein; BPI, base peak intensity; CER, Caerulein; C**1**-C**6**, compounds **1**-**6**; DM, diabetes mellitus; EtOH, ethanol; GPx, glutathione peroxidase; H&E, haematoxylin and eosin; HO-1, haeme oxygenase-1; HRP, horseradish peroxidase; H2-DCFDA, 2,7-dichlorodi-hydrofluorescein diacetate;

IHC, immunohistochemistry; IL-6, Interleukin-6; Keap1, Kelch-like ECH-associated protein 1; MeOH, methanol; MPO, myeloperoxidase; NaT, taurocholic acid sodium salt hydrate; NF-kB, nuclear factor kappa B; Nrf2, nuclear factor erythroid 2-related factor 2; PI, propidium iodide; ROS, reactive oxygen species; SOD, superoxide dismutase; TFE, total flavonoids extraction; TLCS, taurolithocholic acid 3-sulfate disodium salt.

Compounds List: (2R,3R)-taxifolin 7-O-*β*-D-glucopyranoside; (2S)-flavanomarein; (2S)-eriodictyol 7-O-*β*-D-glucopyranoside; (2S)-flavanocorepsin; maritimein; marein.

1. Introduction

Acute pancreatitis (AP) is the commonest pancreatic disease and one of the most common digestive diseases that require emergency hospital admission, with a global increase of incidence (Forsmark et al., 2016; Peery et al., 2015; Xiao et al., 2016). While AP in patients with mild attacks is always considered to be uneventful, moderate to severe cases are often associated with significant compilations that may require surgical intervention and/or organ support (Banks et al., 2013). Despite recent advances in understanding of the pathogenesis and improvement of the management of AP (van Dijk et al., 2017), there is still no specific pharmacological therapy (Moggia et al., 2017).

The important role of oxidative stress in the pathogenesis and progression of various of diseases including AP is well established (Leung and Chan, 2009). Increased oxidative stress includes an array of intermediates such as reactive oxygen species (ROS) and reactive nitrogen species that have been observed in bile acid-, ductal ligation-, caerulein- and amino acid-induced AP animal models (Leung and Chan, 2009). In parallel, pancreatic and serum levels of antioxidant-scavenging enzymes such as glutathione peroxidase (GPx), superoxide dismutase (SOD) and catalase are reduced (Leung and Chan, 2009). The oxidative intermediates cause mitochondrial membrane depolarisation, lipid peroxidation, protein modification and DNA fragmentation in pancreatic acinar cells, leading to ATP deletion and necrosis (Booth et al.,

2011a; Hackert and Werner, 2011); they also switch on proinflammatory signalling pathways by involving mitogen-activated protein kinases, nuclear factor kappa B (NF-kB) and activator protein-1, all of which are key mediators of the inflammatory cascade during AP (Huang et al., 2016; Leung and Chan, 2009).

The nuclear factor erythroid 2–related factor 2 (Nrf2), a member of NF-E2 family of nuclear basic leucine zipper transcription factors, induces activation of antioxidant response elements (AREs) that regulate gene expression of a number of enzymes including GPx, SOD and haeme oxygenase-1 (HO-1) that detoxify oxidative intermediates (Hybertson et al., 2011; Ma, 2013). Under normal conditions, Nrf2 is constitutively degraded by its suppressor Kelch-like ECH-associated protein 1 (Keap1), which binds to the Nrf2 inhibitory Neh2 domain in the cytosol (Ma, 2013). Under stress conditions, Keap1 is degraded to release Nrf2 that translocates into the nucleus, allowing the activation of AREs thus to execute its antioxidant defence function (Ma, 2013). Nrf2 suppression in both the pancreas (Dong et al., 2016; Jung et al., 2010; Robles et al., 2016) and lung (Wang et al., 2014; Yu et al., 2016) has been implicated in murine AP models and correlates with disease severity, while its pharmacological activation reduces disease severity (Dong et al., 2016; Robles et al., 2016).

A large number of compounds of plant origin including polyphenols, terpenes,

glycosides, quinones and flavonoids have been explored for treating a variety of pancreatic disorders including diabetes mellitus (DM) and AP (Anchi et al., 2017). Flavonoids are richly available in large number of vegetables, fruits, tea and herb and the protective mechanisms against AP at least involve antioxidant and anti-inflammatory properties acting on Nrf2 and NF-kB pathways (Shapiro et al., 2007). *Coreopsis tinctoria* Nutt (Asteraceae; also called snow chrysanthemum) is a plant native to North America that has spread worldwide. It has been used to treat several diseases including DM, diarrhoea and internal pain in North America, Portugal and China (Dias et al., 2010; Foster and Duke, 1990; Cui and Ran, 1993; D'Oliveira Feijão R., 1973). Recently, it has been reported that *C. tinctoria* has antidiabetic (Dias et al., 2010) and antioxidant (Chen et al., 2016; Wang et al., 2015) activities that have been attributed to its flavonoid components. As we all known, both AP and diabetes are pancreatic disorder related disease. Emerging evidence suggests that insulin protects against pancreatic toxin-induced acinar cell injury. (Samad et al., 2014) In parallel, flavonoids from *C. tinctoria* could improve insulin sensitivity. (Jiang et al., 2015.) These suggest flavonoids from *C. tinctoria* might be used to target AP.

The aim of this study was to investigate the potential protective effects of leading flavonoids isolated from *C. tinctoria* against AP *in vitro* and *in vivo*. We first used an LC-MS based online technique to analyse and isolate targeted flavonoids. Then we tested these flavonoids on necrotic cell death activation in

freshly isolated acinar cells and further applied them to three different murine AP models. Lastly, we examined whether the protective effects of *C. tinctoria* was at least in part via modulation of Nrf2/ARE-mediated antioxidant signalling pathways.

2. Materials and methods

2.1. Animals and reagents

Male Balb/C mice (25–30 g) and male Wistar rats (250–300 g) were purchased from Chengdu Dossy Experimental Animals Co. LTD (Sichuan, China). Male C57/BL6J mice (25–30 g) were purchased from Beijing Huafukang Bioscience Co. LTD (Beijing, China). Animals were maintained at 22 ± 2°C and exposed to a 12 h light-dark cycle, fed with standard laboratory chow and water, allowed to acclimatise for a minimum of one week. Animals were fasted for 12 h before induction of AP and food was resumed 1 hour after the initial procedure. All animal experiments were approved by the Ethics Committee of West China Hospital of Sichuan University (2017065A).

Acetonitrile and methanol (MeOH) were from Fisher Scientific (Pittsburgh, PA, USA). Hoechest33342, propidium iodide (PI) and 2,7-dichlorodi-hydrofluorescein diacetate (H2-DCFDA) were from Molecular Probes (Eugene, Oregon, USA). Caerulein and taurolithocholic acid 3-sulfate disodium salt (TLCS) were from Sigma-Aldrich (St. Louis, MO, USA). Antibodies against Nrf2 and HO-1 were from Abcam (Cambridge, MA, USA). Antibody against NF-κB p65 was from Cell Signalling Technology (Danvers, MA, USA). Commercial kits for GPx and SOD were purchased from Nanjing Jiancheng Bioengineering Institute (Nanjing, Jiangsu, China). Interleukin-6 (IL-6) ELISA kit was from Abcam (Cambridge, UK). If not otherwise stated, all the other chemical

reagents were purchased from J&K with highest analytical grade (Beijing, China).

2.2. Isolation and analysis of flavonoids from C. tinctoria

The capitula of *C. tinctoria* were from the research base of Uighur Autonomous Region Institute of Medicinal Plants (Xinjiang, China). A voucher specimen (No. 201209) was preserved in the herbarium of Laboratory of Ethnopharmacology of West China Hospital, Sichuan University. The simplified procedure of isolating total flavonoids extraction (TFE) and compounds **1-6** is described in Supplementary Figure S-1. The dried capitula (5 kg) of *C. tinctoria* were extracted with 95% ethanol (EtOH) (3 times). After removal of the solvent under reduced pressure at 45°C, the residue (580 g) was directly subjected to polyamide resin column chromatograph, eluting with H_2O, 35% EtOH and 65% EtOH, successively. The fraction (60.5 g) eluted with 35% EtOH was subjected to a Sephadex LH-20 column, eluting with MeOH to afford four fractions. TFE was mainly from Fr.3. It was further subjected to Sephadex LH-20, eluting with 50% MeOH to afford six fractions. Fr. 3-2 was purified by prep. HPLC (10% acetonitrile, 280 nm) to yield compound **1** (C**1**, 320 mg). Fr. 3-6 purified by prep. HPLC (20% acetonitrile, 280 nm) to yield compounds **2** (C**2**, 260 mg), **3** (C**3**, 330 mg), **4** (C**4**, 85 mg), **5** (C**5**, 228 mg), and **6** (C**6**, 370 mg).

The TFE was analysed on a UPLC I-Class (Waters ACQUITY, Miford, USA) coupled with a QTOF (Xevo G2-XS, Waters, Miford, USA). The separation was

performed on a HSS T3 column (2.1 × 100 mm, 1.8 μm) at 45°C. Gradient elution of 0.1% formic acid solution (Solvent A) and 0.1% formic acid acetonitrile solution (Solvent B) at a flow rate of 0.5 mL/min was employed: 0-0.2 min, 1% B; 0.2-8 min, 1-40% B; 8-12 min, 40-99% B; 12-14 min, 99% B; 14-16 min, 99-1% B. The injection volume was 1 μL. The Q-Tof system was operated on an electrospray ion source in negative ion mode. The mass range was set at m/z 50-1200. The capillary voltage was 3.0 KV. The source temperature was 120°C, and desolvation temperature was 350 °C. Cone gas flow and desolvation gas flow were 50 and 800 L/Hr. The data were acquired on MS^E mode, and analysed using a UNIFI 1.8 software.

2.3. Necrosis, ROS and ATP assays

Pancreatic acinar cells were isolated freshly from Balb/c or C57/BL6J mice using a collagenase IV (Worthington Biochemical Corporation, Lakewood, NJ, USA) digestion procedure as previously described (Huang et al., 2014). Cells were treated under room temperature, and used within 4 hours after isolation. Cells were treated with 5 mM taurocholic acid sodium salt hydrate (NaT) with or without different extracts (1 mM) or various concentrations of C**1** for 30 min, gently shaken at 50 rpm at room temperature to assess necrotic cell death pathway activation. The cells were washed and then stained with Hoechst 33342 (50 μg/ml) and PI (1 μM). Images were taken by fluorescence microscopy ZEISS AX10 imager A2/AX10 cam HRC (Jena GmbH, Germany).

Data were calculated as PI stained cells divided by Hoechst 33342 stained cells and multiplied by 100%.

The cells were first incubated with a ROS indicator H2-DCFDA (Booth et al., 2011b) for 20 min at 37°C in the dark. Then they were distributed into a 96-well glass black plates. The fluorescence was recorded on a Synergy Mx multifunctional Microplate Reader (Gene Company Ltd, Hong Kong, China) for 30 min in total: the baseline was recorded for the first 5 min; after adding 0.5 mM of C**1**, the fluorescence values were recorded for a second 5 min; after adding 5 mM of NaT, the fluorescence values were recorded for the last 20 min. The data of ROS quantification were expressed as F/F_0 and quantified as the $\Delta F/F_0$ at 2250 s for all the groups.

In separate experiments, 5 mM of NaT was added to the acinar cells with and without 0.5 mM of C**1**. After 20 and 40 minutes, the cells were re-suspended in a lysis buffer, boiled for 2 min, and centrifuged at 12,000 g for 5 min. The luminescence of the supernatant of each sample was measured by the Microplate Reader. The data were normalised to protein concentration counted by bicinchoninic acid protein (BCA) assay (Thermo Fisher Scientific, Waltham, MA, USA).

2.4. Induction of AP models and administration of C1

Three AP models were used: (1) mice received seven intraperitoneal injections of a cholecystokinin analog caerulein (Saluja et al., 2007) at hourly interval to

induce hyperstimulation AP (CER-AP) (Huang et al., 2017a; Mukherjee et al., 2016; Wen et al., 2015); (2) mice received retrograde pancreatic ductal injection of 5 mM TLCS (50 μL) to induced biliary AP (TLCS-AP) (Perides et al., 2010); (3) rats received retrograde pancreatic ductal injection of 3.5% NaT (1mL/kg) to induce biliary AP (NaT-AP) (Wan et al., 2012).

Control mice received equivalent volume saline injections, while control mice or rats received sham operation without perfusion of TLCS or NaT. In the CER-AP, C**1** (12.5, 25, and 50 mg/kg) was administered at 0, 4, and 8 hours after the first injection of caerulein and mice in all groups were sacrificed at 12 hours; in the TLCS-AP and NaT-AP, C1 of 12.5 mg/kg or 8.7 mg/kg (equivalent to 12.5 mg/kg in the mice) was administered at 0, 4, and 8 hours post-operation and all animals were sacrificed at 24 hours. Pancreas, lung and blood samples were collected for disease severity assessment and mechanistic study.

2.5. Histopathology and immunohistochemistry (IHC)

Pancreas samples were fixed in 10% buffered formaldehyde embedded in paraffin, sectioned in 5 mm and stained with haematoxylin and eosin (H&E). Pancreatic histopathology (magnification × 200) were scored independently by two pathologists who were unware of the study design. Criteria were oedema, inflammatory cell infiltration and necrosis with each component having a score of 0 to 3 as previously described (Wildi et al., 2007). For assessing pancreatic histopathology in the TLCS-AP, a 4-point scoring system for each component

(oedema, inflammatory cell infiltration and necrosis) was used without scoring haemorrhage (Zhou and Xue, 2009). Immunostaining was performed on 4 μm-thick sections after deparaffinisation. Microwave antigen retrieval was performed in citrate buffer (pH 6.0) for 10 min prior to peroxidase quenching with 3% H_2O_2 in MeOH for 10 min. Sections were then washed in water and preblocked with normal goat serum for 10 min. In the primary antibody reaction, slides were incubated for 1 hour at room temperature in a 1:100 dilution of antibody. The sections were then incubated with biotinylated secondary antibodies (1:1000) for 1 hour. Following a washing step with phosphate-buffered saline, streptavidin-horseradish peroxidase (HRP) was applied. Finally, the sections were developed with diaminobenzidine tetrahydrochloride substrate for 5 min, and counterstained with hematoxylin. Each section was scanned using NanoZoomer 2.0 HT from HAMAMATSU Photonics (Hamamatsu, Japan), and analysed by Image-Pro Plus 6.0 (Rockville, MD, USA).

2.6. Measurement of trypsin and myeloperoxidase (MPO) activity

The detailed methodology of measuring trypsin and MPO activity was described as previously (Huang et al., 2017a; Huang et al., 2017b).

2.7. Determination of serum amylase, lipase and IL-6 levels

Serum amylase and lipase were measured using a full automatic biochemical analyser (Roche, Mannheim, Germany). IL-6 levels were evaluated by an

ELISA kit according to the manufacturer's instructions.

2.8. Determination of pancreatic GPx and SOD levels

Pancreatic GPx and SOD levels in homogenised pancreas tissue were measured using commercial kits as described (Dong et al., 2016).

2.9. Western-blot analysis

The pancreatic tissue was pulverised after being snap-frozen in liquid nitrogen. Total protein was extracted by adding a cocktail (phosphate inhibitor, phenylmethylsulfonyl fluoride and protease inhibitor) at the proportion of 1 μg tissue per 10 μL cocktail. Total protein concentration was quantified using a BCA kit. A 30 μg aliquot of protein or equal proportion of concentrated supernatant was subjected to sodium dodecyl sulphate/polyacrylamide gel electrophoresis (Bio-Rad, CA, USA) and transferred to nitrocellulose/polyvinylidene fluoride membrane following the standard method. Membranes were blocked with 5% non-fat milk at room temperature for 1 hour and were further incubated overnight at 4°C with primary antibodies. β-actin was used as the internal reference for proteins. Membranes were washed with a mixture of tris-buffered saline and polysorbate 20 and incubated with a secondary goat anti-rabbit IgG-HRP antibody (1:5000) or goat anti-mouse IgG-HRP antibody (1:10000) (Proteintech, Wuhan, Hubei, China) for 1 hour at room temperature. Finally, membranes were washed and developed using the detection system (Bio-Rad, Hercules, CA, USA).

2.10. Statistical analysis

Statistical analysis was performed using ANOVA and an unpaired Student's t-test. A *P*-value of < 0.05 was taken to indicate statistical significance. Statistical calculations were performed using SPSS software for Windows (Version 21.0; SPSS, Chicago, IL, USA).

3. Results

3.1. LC/MS analysis of TFE from C. tinctoria and identification of the C1 - C6

The TFE was purified from EtOH extract of *C. tinctoria* by multiple column chromatography. The TFE was first detected under the negative mode by UPLC-QTof/MS (Figure 1). The peaks in the base peak intensity (BPI) chromatograph of TFE were identified as 19 flavonoids by comparing MS data with data base, the components were listed in Supplementary Table S-1. Thereof, peaks 1-6 were targetedly isolated from the TFE, and determined to be (2R,3R)-taxifolin 7-O-*β*-D-glucopyranoside (C**1**), (2S)-flavanomarein (C**2**), (2S)-eriodictyol 7-O-*β*-D-glucopyranoside (C**3**), (2S)-flavanocorepsin (C**4**), maritimein (C**5**) and marein (C**6**) by comparisons with references. (Supplementary Figures S2-7)

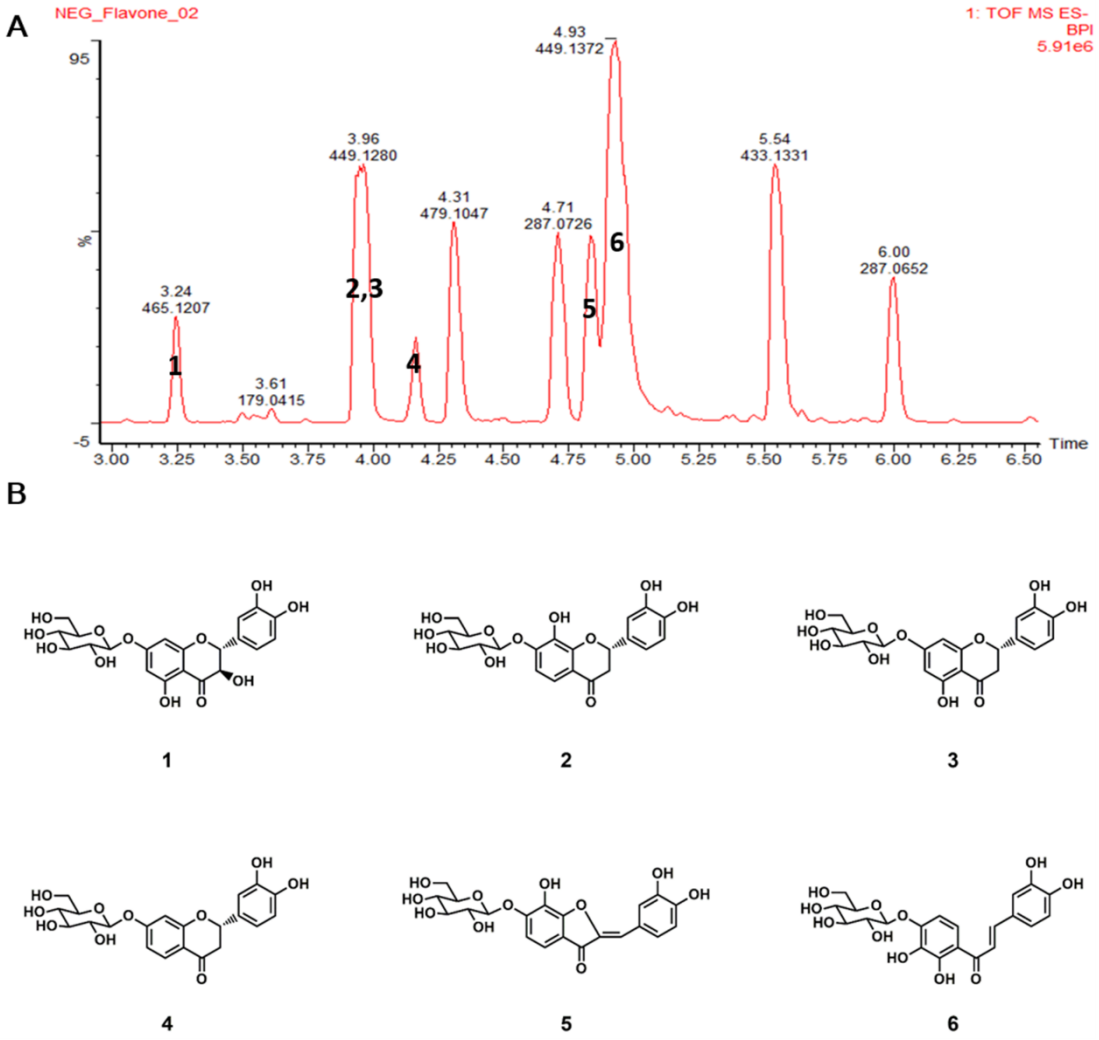

Fig. 1. Representative base peak intensity (BPI) chromatogram of total flavonoids extract (TFE) isolated from *C. tinctoria* and structures of compounds **1**-**6** (C**1**-C**6**) isolated from TFE. (A) BPI chromatograms were monitored in negative ion mode. (B) C**1**-C**6** were identified as (2R,3R)-taxifolin 7-O-*β*-D-glucopyranoside (C**1**), (2S)-flavanomarein (C**2**), (2S)-eriodictyol 7-O-*β*-D-glucopyranoside (C**3**), (2S)-flavanocorepsin (C**4**), maritimein (C**5**) and marein (C**6**).

3.2. C1 showed the strongest protective effect in reducing necrotic cell death pathway activation

The effects of extracts (1 mM) prior to TFE on necrotic cell death pathway activation in acinar cells induced by NaT (5 mM) are shown in Supplementary Figures S-8, while the effects of TFE and C**1**-C**6** (1 mM) are shown in Figure 2A. The control cells had a baseline PI uptake around 20%, this was dramatically increased after the application of 5 mM NaT (normalised to 100%). NaT-induced PI uptake was reduced in total extract and 3 out of 4 extracts from the 35% EtOH extract, but not H_2O extract or 65% EtOH extract. NaT-induced PI uptake was reduced to below 50% by C**1**-C**4** with the best effect achieved by C**1** (28%), while no significant alterations were observed by TFE or C**5**; there was a trend towards a reduction by C**6**, but this did not reach statistical significance. We further explored the effects of different concentrations (0.25, 0.5 and 1 mM) of C**1**, a flavanonol, on necrotic cell death pathway activation (Figure 2B). While a more reduced PI uptake was observed at 0.5 mM, there was no significant difference among different concentration used.

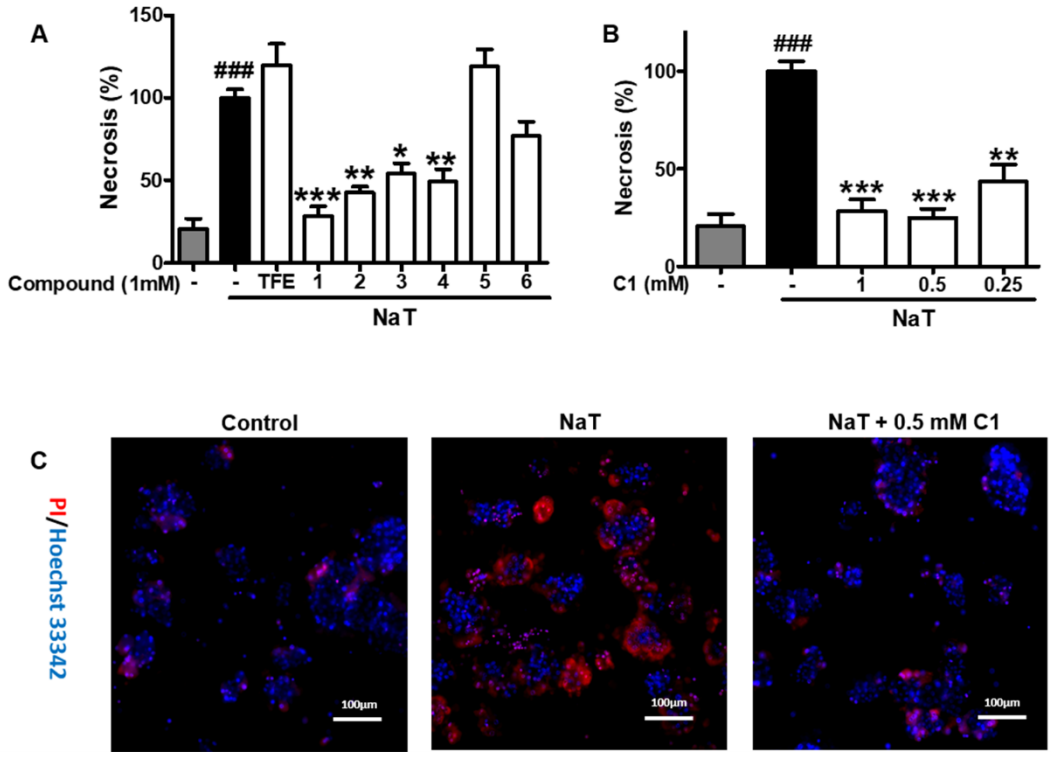

Fig. 2. Effects of flavonoids isolated from *C. tinctoria* on necrotic cell death activation in mouse pancreatic acinar cells. Cells were treated with normal saline or taurocholic acid sodium salt hydrate (NaT, 5 mM) with or without compounds at designated concentrations. The necrosis % (PI uptake) induced by NaT was calculated from Hoechst 33342 stained cells and multiply by 100 %. (A) Effects of TFE and C**1**-C**6** at the concentration of 1 mM. (B) Effects of C**1** at the concentration of 0.25, 0.5 and 1 mM. (C) Representative images showing Hoechst 33342 (*blue*) and PI (*red*) stained with cells treated with normal saline, NaT, and NaT + C**1** (0.5 mM). Data are expressed as mean ± SEM from 3 or more independent experiments. $^{*}P < 0.05$, $^{**}P < 0.01$, and $^{***}P < 0.001$ vs. model group, $^{###}P < 0.001$ vs. control group. In the histogram: *dark grey* = control, *black* = NaT, and *white* = NaT with treatment (TFE or C**1**-C**6**).

3.3. C1 reduced ROS production and ATP depletion

The inhibitory effects of C**1** on ROS production by NaT (5 mM) were investigated (Figure 3A(i)). There was a sustained increase of ROS reflected by fluorescence intensity of H2-DCFDA followed stimulation with NaT (1.41), which was reduced to 1.13 by C**1** application, and the absolute difference was significant (0.38 vs. 0.11, $P < 0.001$; Figure 3A(ii)). In line with this, NaT induced marked ATP depletion at 20 and 40 mins; these were significantly reverted by application of C**1** (48% vs. 64% at 20 mins; 18% vs. 26% at 40 mins; both $P < 0.001$; Figure 3B). These data collectively suggest that the protective effects of C**1** on necrotic cell death pathway in acinar cells at least in part were mediated by inhibition of ROS production to preserve ATP levels.

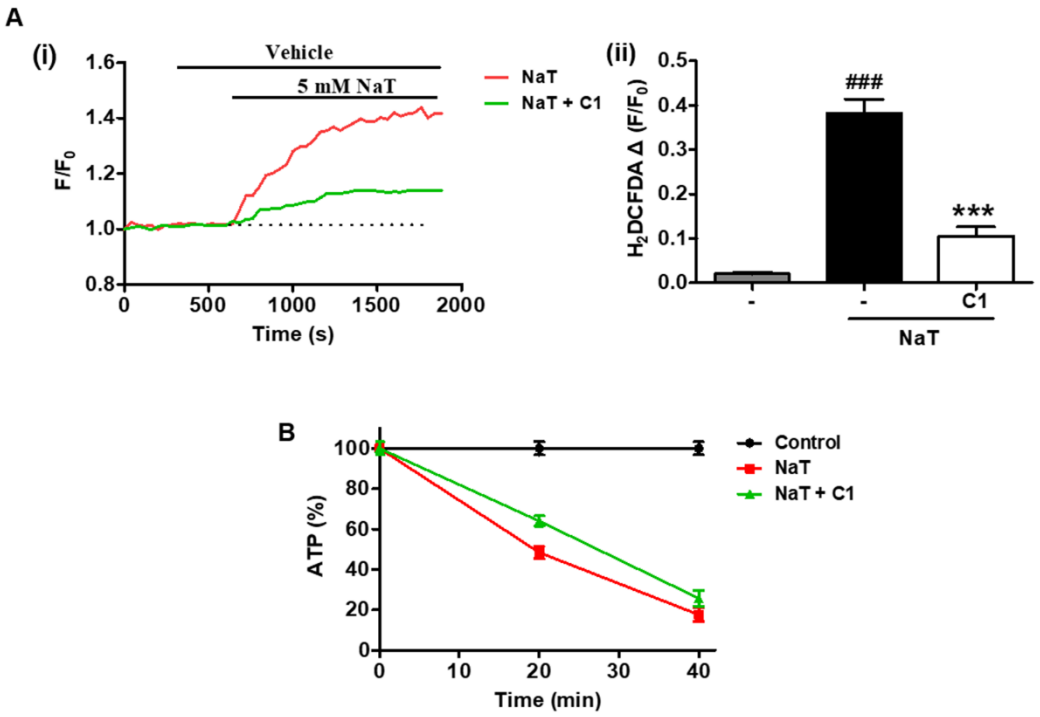

Fig. 3. Effects of C**1** on ROS production and ATP depletion in mouse pancreatic acinar cells. Cells were treated with normal saline or taurocholic acid sodium salt hydrate (NaT, 5 mM) with or without C**1** (0.5 mM). ROS was measured by fluorescent H2-DCFDA and ATP was tested by luminescence. (A) Typical traces NaT-induced ROS production which was suppressed by C**1** administration. (B) Summary quantification of ROS production. (C) The inhibition effect of C**1** on ATP deletion. Data are normalised to the control as 100%. Data are expressed as the means ± SEM from 3 or more independent experiments. $^{***}P < 0.001$ vs. NaT group, $^{###}P < 0.001$ vs. control group. In the histogram: *dark grey* = control, *black* = NaT, and *white* = NaT with C**1**.

3.4. C1 reduced local and systemic complications in experimental AP models

Oral gavage C**1** was not as effective as intraperitoneal injections in the CER-AP, thus the latter approach was used throughout *in vivo* studies. The effects of C**1** on CER-AP and NaT-AP are shown in Figures 4 and 5, respectively. Hyperstimulation and retrospective pancreatic duct perfusion of NaT all caused typical histopathological features of AP - marked oedema, inflammatory cell infiltration and acinar cell necrosis (Huang et al., 2014; Huang et al., 2017a; Huang et al., 2017b; Mukherjee et al., 2016; Wen et al., 2015; Zhang et al., 2016); these changes were also reflected by a dramatic increase of serum amylase and lipase, parameters to diagnose AP in clinical settings (Banks et al., 2013); pancreatic trypsin (not assessed in the NaT-AP) and MPO activities were increased which represented intrapancreatic digestive enzyme activation (Dawra et al., 2011) and neutrophil infiltration (Dawra et al., 2008), respectively; lung MPO and serum IL-6 levels were characteristics of systemic inflammation which were consistently elevated in both models employed.

In the CER-AP, C**1** at a lower dose (12.5 mg/kg) greatly improved pancreatic morphology (Figure 4A(i)) and halved the overall histopathological score (Figure 4A(ii)) with profound effects on reducing inflammatory cell infiltration (Figure 4A(iv)) and necrosis (Figure 4A(v)), but not oedema (Figure 4A(iii)). Similarly, C**1** significantly reduced serum amylase (Figure 4B) and lipase

(Figure 4C), pancreatic trypsin (Figure 4D) and MPO (Figure 4E). In accordance with local injury, systemic injury markers lung MPO (Figure 4F) and serum IL-6 (Figure 4G) were also significantly decreased. The protective effects of C**1** at higher doses (25 and 50 mg/kg) were inconsistent.

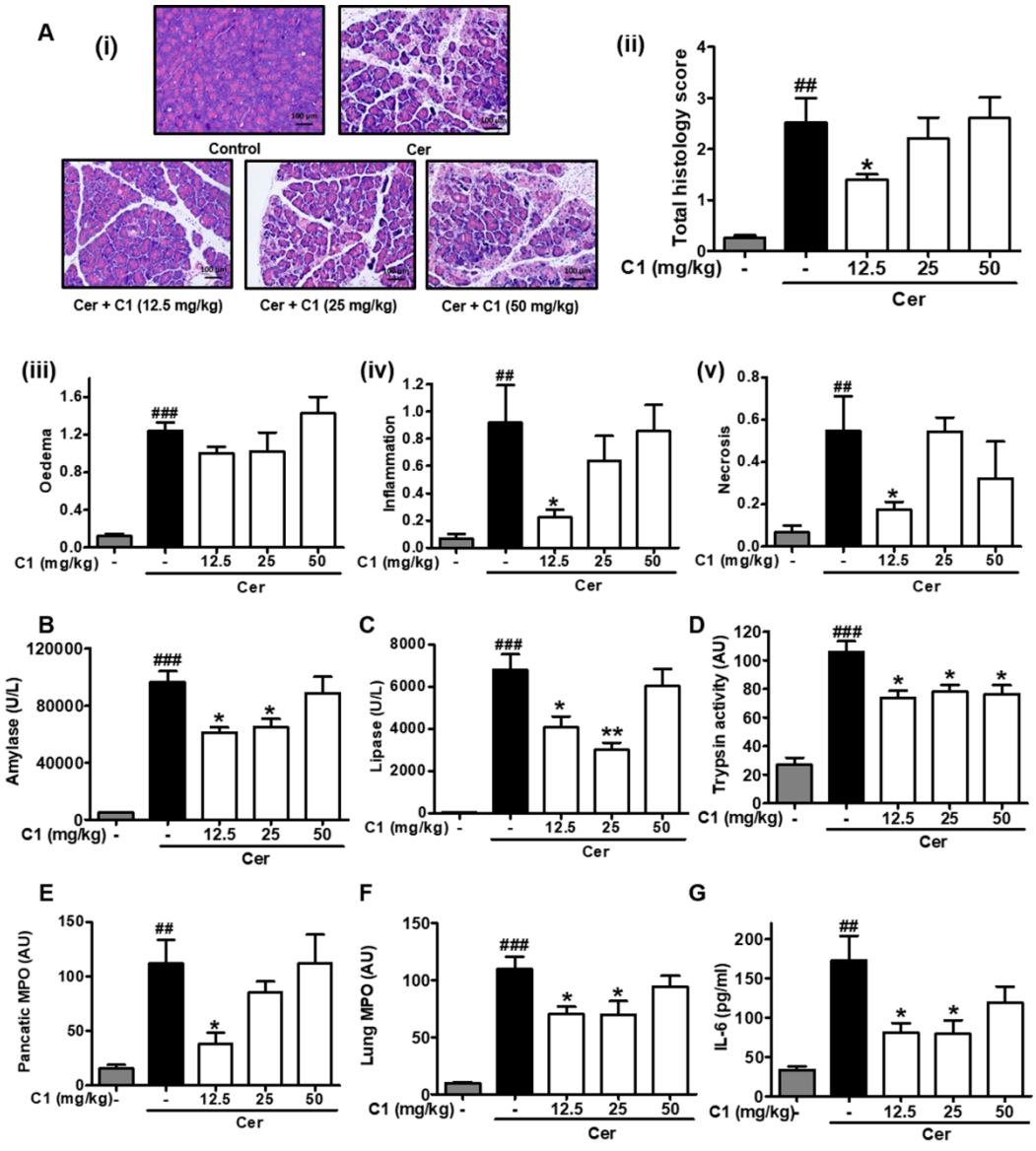

Fig. 4. Effects of C**1** on severity of caerulein-induced acute pancreatitis (CER-AP) in mice. CER-AP was induced by 7 intraperitoneal injections of caerulein (Cer) at hourly interval, while control mice received saline injections. In the treatment group, mice received intraperitoneal injections of C**1** (12.5, 25 and 50 mg/kg) at 0, 4 and 8 hours from the first injection of caerulein. All mice were sacrificed at 12 hours after first caerulein/saline injection. (A) C**1** reduced pancreatic histopathology damage: (i) representative haematoxylin and eosin

(H&E) sections of pancreas from control, Cer and Cer with C**1**. (ii) overall histopathology score and its breakdown scores - (iii) oedema, (iv) inflammation and (v) necrosis. (B) Serum amylase. (C) Serum lipase. (D) Pancreatic trypsin activity. (E) Pancreatic myeloperoxidase (MPO) activity. (F) Lung MPO activity and (G) serum interleukin-6 (IL-6) levels. Data are expressed as means ± SEM from 6 or more animals per each group. $^{*}P < 0.05$ and $^{**}P < 0.01$ vs. Cer group, $^{\#\#}P < 0.01$ and $^{\#\#\#}P < 0.001$ vs. control group. In the histogram: *dark grey* = control, *black* = Cer, and *white* = Cer with C**1** at different doses.

Informed by CER-AP, we used a lower concentration of C**1** in the TLCS-AP (12.5 mg/kg) and NaT-AP (8.7 mg/kg; equivalent to 12.5 mg/kg in mice). C**1** significantly reduced overall histopathological score and breakdown scores as well as serum amylase and lipase (Supplementary Figure S-9A-9C). In agreement with these findings, C**1** consistently improved pancreatic morphology (Figure 5A(i)), significantly reduced overall histopathological score (Figure 5A(ii)) and its breakdown scores: oedema (Figure 5A(iii)), inflammation score (Figure 5A(iv)) and necrosis (Figure 5A(v)). Serum amylase (Figure 5B) and lipase (Figure 5C), pancreatic MPO (Figure 5D), lung MPO (Figure 5E) and serum IL-6 (Figure 5F) were also invariably decreased.

All the data obtained from *in vivo* studies suggest that C**1** from the *C. tinctoria* has therapeutic potential for human AP and it is valuable to understand its mechanisms.

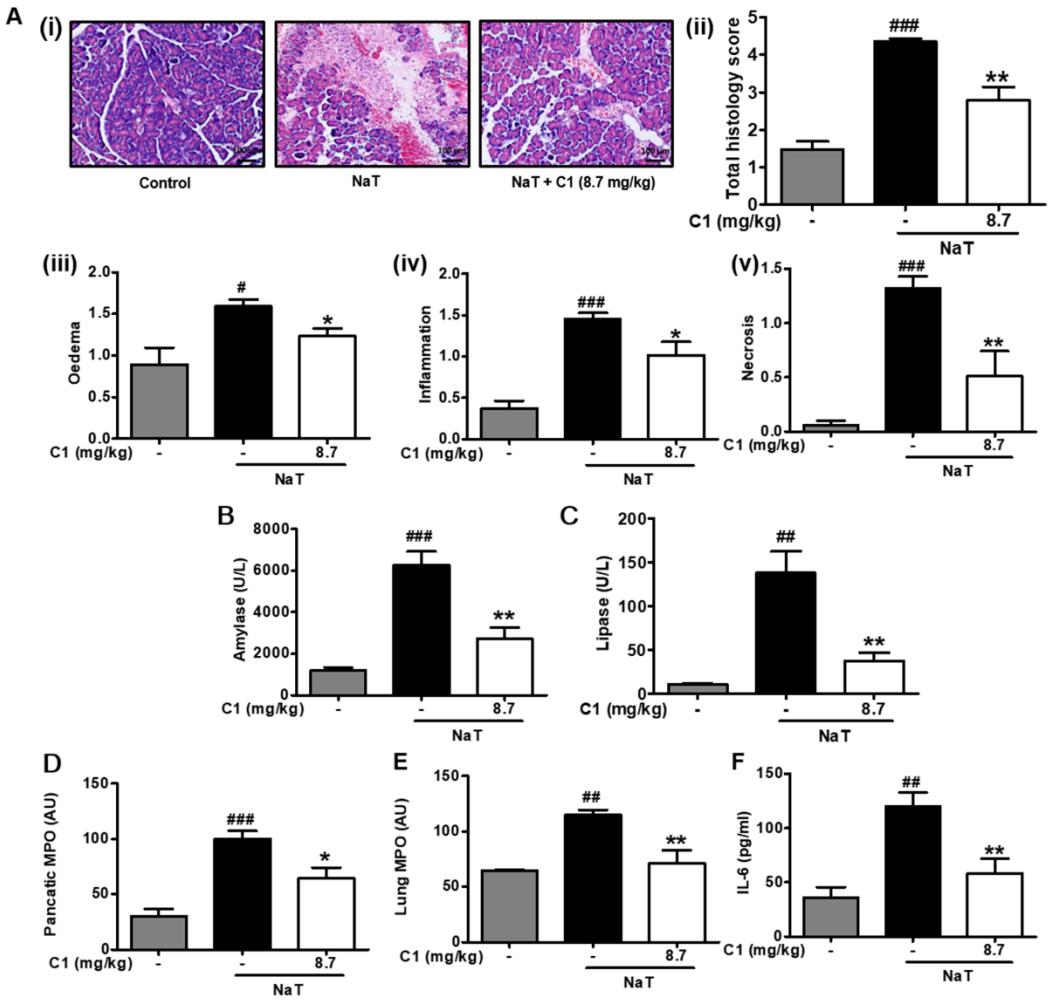

Fig. 5. Effects of C**1** on severity of bile acid-induced acute pancreatitis (NaT-AP) in rats. NaT-AP was induced by retrograde infusion of 3.5% taurocholic acid sodium salt hydrate into the pancreatic duct, while control rats received sham operation. In the treatment group, rats received intraperitoneal injections of C**1** (8.7 mg/kg; equivalent to 12.5 mg/kg in mice) at 0, 4 and 8 hours post-operation. All rats were sacrificed at 24 hours post-operation. (A) C**1** reduced pancreatic histopathology damage: (i) representative haematoxylin and eosin (H&E) sections of pancreas from control, NaT, and NaT with C**1**. (ii) overall histopathology score and its breakdown scores - (iii) oedema, (iv) inflammation and (v) necrosis. (B) Serum amylase. (C) Serum lipase. (D) Pancreatic

myeloperoxidase (MPO) activity. (E) Lung MPO activity and (F) serum interleukin-6 (IL-6) levels. Data are expressed as means ± SEM from 6 or more animals per each group. $^{*}P < 0.05$ and $^{**}P < 0.01$ vs. NaT group, $^{\#}P < 0.05$, $^{\#\#}P < 0.01$ and $^{\#\#\#}P < 0.001$ vs. control group. In the histogram: *dark grey* = control, *black* = NaT, and *white* = NaT with C**1**.

3.5. C1 up-regulated pancreatic Nrf2 protein

Since *C. tinctoria* is well known for its antioxidant effects (Chen et al., 2016; Dias et al., 2010), we hypothesised that the protective effects offered by C**1** were at least operating in part through this mechanism. Moreover, Nrf2/ARE-mediated antioxidant signalling pathway represents one of the most important cellular defence mechanisms against oxidative stress, and we examined the levels of pancreatic Nrf2 and NF-κB p65 protein expression, and Nrf2 targeted stress response protein HO-1 and antioxidant enzymes (GPx and SOD). Representative IHC images of Nrf2 staining are shown in Figure 6A. There was scattered staining in the cytosol but no discernible staining in the nucleus of saline controls; marked staining in both cytosol and nucleus was observed in the caerulein treated group; C**1** at all doses increased the overall expression of Nrf2 protein with most marked effect achieved by 12.5 mg/kg. To further confirm these findings, Western-blot analysis of Nrf2 protein from the pancreatic tissue lysate was conducted. Representative Western-blot images of Nrf2 protein are displayed in Figure 6B. The trend of Nrf2 protein expression was in line with the IHC findings. Quantitative Western-blot analysis revealed that the Nrf2 protein in the caerulein group was significantly higher, compared with the saline group, while C**1** treated groups were even higher with only the low dose group (12.5 mg/kg) reaching statistical significance compared with caerulein (Figure 6C). The findings of pancreatic Nrf2 protein expression were mirrored by the NF-κB p65 (Figure 6D). It is shown that caerulein administration increased pancreatic

NF-κB p65 compared with saline injections, while C**1** treatment reduced caerulein-induced NF-κB p65 activation (Figure 6E). However, no statistical significance was reached between groups of designated comparison.

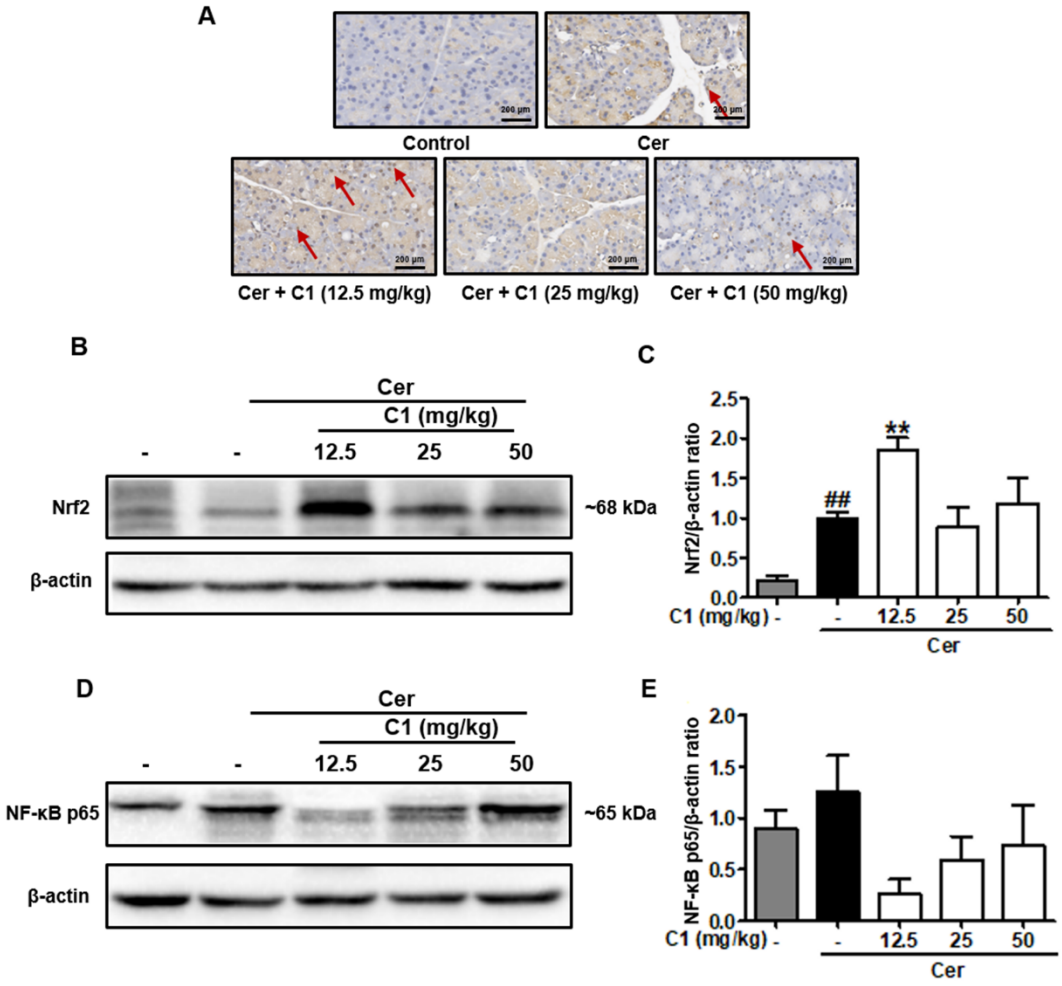

Fig. 6. Effects of C**1** on pancreatic Nrf2 and NF-κB (p65) expressions in caerulein-induced acute pancreatitis (CER-AP) in mice. CER-AP was induced by 7 intraperitoneal injections of caerulein (Cer) at hourly interval, while control mice received saline injections. In the treatment group, mice received intraperitoneal injections of C**1** (12.5, 25 and 50 mg/kg) at 0, 4 and 8 hours from the first injection of caerulein. All mice were sacrificed at 12 hours after first caerulein/saline injection. Pancreatic tissues were homogenised for immunohistochemistry and Western-blot analysis of Nrf2 and NF-κB p65 protein expression. (A) Representative immunohistochemistry images from

control, Cer, and Cer with C**1** (red arrow indicates Nrf2 nuclear translocation). (B) Representative Western-blot images for Nrf2 from control, Cer, and Cer with C**1**. (C) Quantification of Western-blot images for Nrf2. (D) Representative Western-blot images for NF-κB p65 from control, Cer, and Cer with C**1**. (E) Quantification of Western-blot images for NF-κB p65. Data are expressed as means ± SEM from 4 or more animals per each group.$^{**}P< 0.01$ vs. Cer group, $^{\#\#}P < 0.01$ vs. control group. In the histogram: *dark grey* = control, *black* = Cer, and *white* = Cer with C**1** at different doses.

3.6. C1 increased the pancreatic Nrf2-targeted stress response protein HO-1 and antioxidant enzymes GPx and SOD

The IHC and Western-blots images as well as Western-blot quantification of HO-1 protein expression are shown in Figure 7A, B and C, respectively. These data are in agreement with the Nrf2 protein expression profile that the HO-1 protein expression was: C**1** (12.5 mg/kg) treated > caerulein alone > saline controls.

Consistent with published literature (Leung and Chan, 2009), the pancreatic antioxidant enzymes GPx (Figure 7D) and SOD (Figure 7E) were significantly reduced after caerulein challenge. In accord with C**1** activation of the Nrf2/ARE antioxidant signalling pathways, C**1** at low to moderate doses (12.5 and 25 mg/kg) increased pancreatic GPx (Figure 7D) and SOD (Figure 7E) levels, albeit a statistical significance was not reached by C**1** at 12.5 mg/kg for SOD. However, C**1** at 50 mg/kg was ineffective.

These data of C**1** on pancreatic Nrf2, HO-1, GPx and SOD collectively suggest that C**1** may reduce severity of AP by promoting pancreatic antioxidant enzyme generation via activation of Nrf2/ARE pathways.

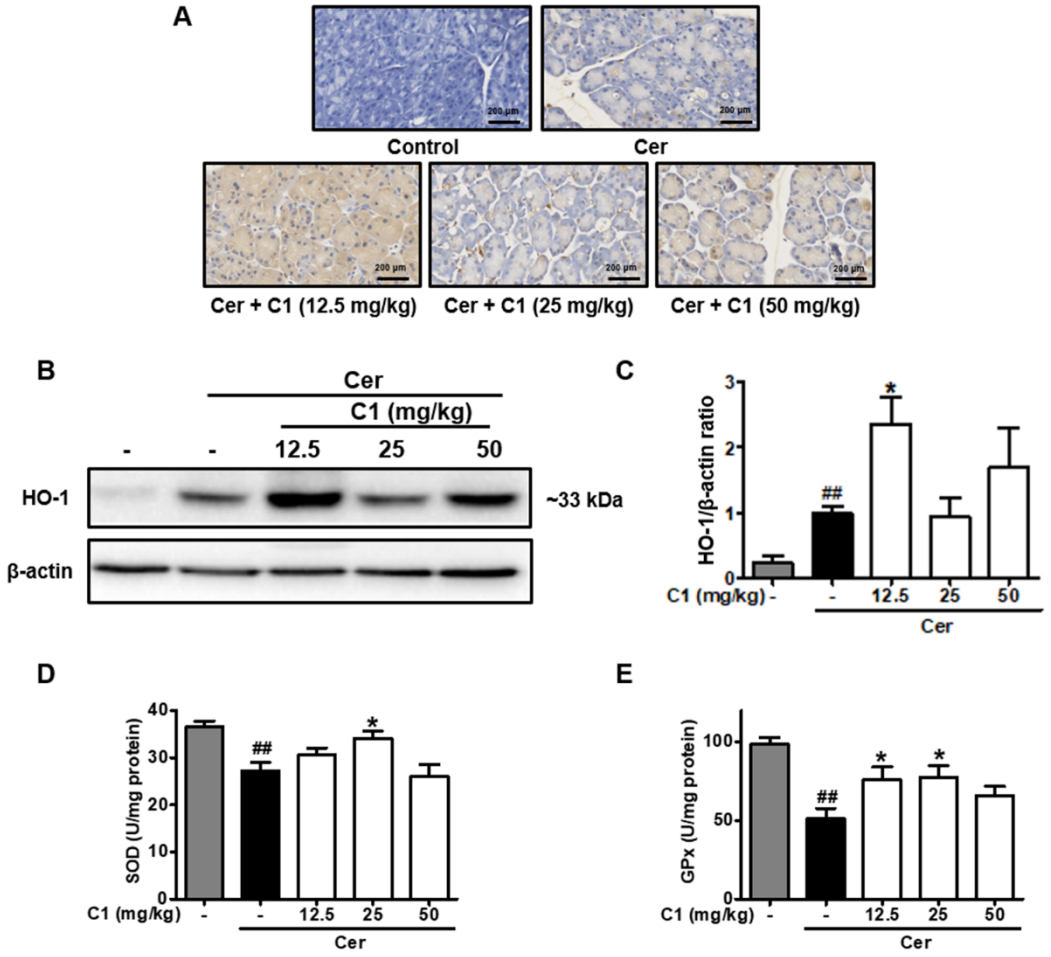

Fig. 7. Effects of C**1** on pancreatic Nrf2/ARE-mediated signalling pathways in caerulein-induced acute pancreatitis (CER-AP) in mice. CER-AP was induced by 7 intraperitoneal injections of caerulein (Cer) at hourly interval, while control mice received saline injections. In the treatment group, mice received intraperitoneal injections of C**1** (12.5, 25 and 50 mg/kg) at 0, 4 and 8 hours from the first injection of caerulein. All mice were sacrificed at 12 hours after first caerulein/saline injection. Pancreatic tissues were homogenised for immunohistochemistry and Western-blot analysis of HO-1 protein expression as well as to test GPx and SOD levels. (A) Representative immunohistochemistry images from control, Cer, and Cer with C**1** for HO-1. (B)

Representative Western-blot images from control, Cer and Cer with C**1**. (C) Quantification of Western-blot images for HO-1. (D) GPx and (E) SOD. Data are expressed as means ± SEM from 4 or more animals per each group. *P < 0.05 vs. Cer group, $^{\#\#}P$ < 0.01 vs. control group. In the histogram: *dark grey* = control, *black* = Cer, and *white* = Cer with C**1** at different doses.

4. Discussion

In this study, we successfully used LC-MS to isolate targeted flavonoids from *C. tinctoria*, a well-known flower tea material having antioxidant properties that is used world-wide (Chen et al., 2016). For the first time we tested these flavonoids on necrotic cell death pathway activation induced by NaT in acinar cells and identified that C**1** had the best protective effects. Further C**1** was shown to reduce ROS production and prevent ATP depletion in acinar cells. Moreover, using the most widely used (hyperstimulation) and clinical aetiology relevant (bile acid) models, we have shown that C**1** markedly reduced the severity of AP, evidenced by suppressed histopathological, biochemical and immunological parameters for local and systemic complications. Lastly, we found that the pancreatic Nrf2, HO-1, GPx and SOD levels were significantly increased by C**1** treatment when compared to caerulein challenge alone, suggesting a Nrf2/ARE-mediated antioxidant signalling pathway activation in protecting against AP.

Several *in vivo* studies found that natural compounds ameliorate oxidative stress and therefore have therapeutic potential for a various of conditions including inflammatory diseases like AP (Anchi et al., 2017; Shapiro et al., 2007). *C. tinctoria* has been well-known for its antioxidant capacity (Chen et al., 2016; Dias et al., 2010) but there are no studies assessing its effects on AP, a disease in which oxidative stress plays an important role in the pathogenesis

(Booth et al., 2011a; Hackert and Werner, 2011; Leung and Chan, 2009). Phytochemical and pharmacological studies have shown that flavonoids (Chen et al., 2016; Dias et al., 2010) and polyacetylene glycosides (Du et al., 2016; Guo et al., 2017) are the main biological components of *C. tinctoria*. A few dozens of papers have indicated that the flavonoids-rich fraction could increase insulin sensitivity, regulate hepatic metabolism, promote glucose tolerance regain, and protect from liver injury due to the antioxidant activity of flavonoids (Dias et al., 2010; Dias et al., 2012; Jiang et al., 2015; Tsai et al., 2017). Therefore, in this study we isolated targeted flavonoids from *C. tinctoria* and tested their effects towards AP.

In vitro pancreatic acinar cell necrosis model induced by NaT was first used to identify the best protective activity from TFE and flavonoids **1**-**6** (C**1**-C**6**) isolated from *C. tinctoria.* A previous study used 0.4 mM of marein and flavanomarein and showed that these flavonoids attenuated *tert*-butyl hydroperoxide-induced beta-pancreatic MIN6 cell death *in vitro* (Dias et al., 2012). Hence, we started to test the extracted TFE and flavonoids on freshly isolated acinar cells using 1 mM with or without application of NaT. All flavonoids had no effects on cell death *per se*, while C**1**-C**4** significant reduced NaT-induced necrotic cell death pathway activation with C**1** exhibiting the most pronounced protective effects. However, C**5** and C**6** with a pair of naturally and easily inter-convertible isomers, did not significantly protected against pancreatic acinar necrosis at 1 mM. According to the structure-activity

relationship analysis, the protective activities order of isolates C**1**-C**6** are: flavanonol > flavanone > chalcone > nurone. Further dose characterisation of C**1** demonstrated that it reached a maximal inhibitory effect at 0.5 mM among the doses tested. It is known that the bile acid TLCS induced increased ROS production, and excessive ROS was associated with mitochondrial membrane potential depolarisation and ATP depletion (Booth et al., 2011a). In our previous study (Zhang et al., 2016), we have also shown that NaT, the most commonly used bile acid in literature to induce AP (Lerch and Gorelick, 2013; Wan et al., 2012), also caused ROS production, mitochondrial membrane potential depolarisation, ATP depletion and necrotic cell death pathway activation in freshly isolated acinar cells. Flavonoids are regarded as free radical scavengers by donating hydrogen ions to neutralise toxic ROS. (Ma et al., 2016) Thus, 0.5 mM of C**1** was used to evaluate its effect on ROS generation and ATP depletion induced by NaT in acinar cells. Consequently, C**1** prevented excessive ROS production and ATP depletion. Our *in vitro* data are consistent with the protective effects of (2R,3R)-taxifolin 7-O-*β*-D-glucopyranoside (C**1**) on preventing necrotic cell death pathway activation to result from the reduction of oxidative stress. We have not excluded any contribution of C**1** to protection through any other mechanism that might simultaneously alleviate oxidative stress. Nevertheless the increase of Nrf2 and HO-1 expression with NaT and C**1** over both negative (no NaT) and positive (NaT without C**1**) control conditions supports a role for Nrf2.

To demonstrate the protective effects of C**1** on AP injury *in vivo*, we used a regimen of C**1** intraperitoneal administration at 0, 4 and 8 hours from first caerulein injection or post-surgery. Firstly, compared with oral gavage, intraperitoneal injection of C**1** showed better effects to reduce histopathological, biochemical and immunological changes. The injection time interval was referred to pharmacokinetic parameters of C**1** analogue and our previous treatment (Khaled et al., 2003; Yang et al., 2016; Zhang et al., 2016). Normally the half-life of flavonoids and their glycosides are within 2 hours after intravenous injection and within 4 hours after oral dose, thus a 4-hour interval could maintain a reasonable blood concentration of flavonoid metabolites. Lastly, the three doses of 12.5, 25 and 50 mg/kg were chosen according to former studies which indicated that the C**1** analogue quercetin ameliorates AP at 25, 50 and 100 mg/kg at the tested oral doses 1 hour before induction and at 100, 150 and 200 mg/kg by intraperitoneal injection (Carvalho et al., 2010; Zheng et al., 2016).

The summary *in vivo* findings suggest that C**1** at a lower dose (12.5 mg/kg) consistently reduced all the parameters of disease severity, paving the way for further in-depth characterisation of this natural compound as clinically there is no licensed medicine for treating human AP (Moggia et al., 2017). Although clinical trials of anti-oxidants have as yet failed to deliver a licensed therapy (Hackert et al., 2011), the wrong anti-oxidant treatment may have been trialled and/or started too late during the course of AP. Pre-existing DM acerbates the

severity of AP and AP is associated with substantial occurrence of prediabetic and/or DM (Das et al., 2014); C**1** might be used to target AP and DM simultaneously. Furthermore, emerging experimental evidence suggests that insulin protects against pancreatic toxin-induced acinar cell injury by ameliorating pathological calcium signalling, independent of oxidative stress (Mankad et al., 2012; Samad et al., 2014). Since oxidative stress is implicated in DM (Johansen et al., 2005; Maritim et al., 2003), and C**1** counteracts both DM and AP, further studies are warranted to investigate the effects of C**1** on the onset of AP with pre-existing DM and onset of DM after AP. Further work is also required to understand the loss of effect at higher doses of C1, potentially due to interference with redox signalling essential to mitochondrial metabolism (Booth et al., 2011a, 2011b).

Since most of the protective effective of flavonoids are attributed to its antioxidant properties and Nrf2 is one of the most important factors to regulate this, we questioned that C**1** protected against AP via up-regulating Nrf2/ARE. Recently, strategies of up-regulating Nrf2 in both pancreas and lung by natural or synthetic compounds have been shown to reduce the severity of AP (Dong et al., 2016; Jung et al., 2010; Robles et al., 2016; Wang et al., 2014). A variety of small molecule inducers of Nrf2 have been identified from natural sources as well as from synthetic agents. The chemical structures of inducers include Michael acceptors, oxidisable diphenols, isothiocyanates and etc. (Magesh et al., 2012). Up till now, only one study reported that the Nrf2 inducer

sulforaphane, a natural isothiocyanate, attenuated pancreatic damage by exerting antioxidant defensive activities through the Nrf2 pathway (Dong et al., 2016). Among the isolates C**1**-C**6**, C**3** has been used as Nrf2 activator, which was able to stabilise Nrf2 by delaying Nrf2 degradation (Hu et al., 2012). In our study, C**1** treatment induced pancreatic Nrf2 activation and its nuclear translocation in CER-AP, which resulted in significantly elevated HO-1, GPx and SOD compared to CER-AP alone. Interestingly, in contrary to the previous study using CER-AP (Dong et al., 2016), we observed increased cytosolic and nuclear expression of Nrf2 rather than reduced when compared to the saline controls. The reason for this may due to the different time of assessing Nrf2 protein expression. The previous study tested the Nrf2 expression one hour after last injection of caerulein, while we did this a few hours later. It may well be that immediately after caerulein injection the antioxidant capacity was more suppressed since the stimuli still existed. It is worthwhile to conduct experiments to dynamically measure the expression of Nrf2 and Nrf2/ARE-dependent antioxidant enzymes in AP models to understand their changes according to the disease course.

5. Conclusions

The present study, for the first time, has demonstrated protective effects of flavonoids isolated from *C. tinctoria* against AP injury. It is likely that C**1**, the most effective compound, protected against AP both in *vitro* and *in vivo* by its antioxidant property, at least in part via up-regulating Nrf2 and thus the Nrf2/ARE-associated antioxidant enzymes. The results suggest the potential utilisation of *C. tinctoria* to protect pancreatic disorders like AP.

6. Conflict of interest

None of the authors have conflicts to disclose.

7. Authors' contributions

D. Du (dudan1520@163.com), W. Huang (dr_wei_huang@163.com) and R. Sutton (r.sutton@liv.ac.uk) designed the study. D. Du (dudan1520@163.com) and W. Huang (dr_wei_huang@163.com) wrote the manuscript. D. Du (dudan1520@163.com), L. Yao (linbo_yao108@163.com) and R. Zhang (zr900204@126.com) conducted the major experiments. N. Shi (shina1125@163.com), Y. Shen (shenbmy@126.com), X. Yang (xinmin_yang29@163.com), X. Zhang (xiaoying.zhang@liv.ac.uk), L. Hu (wery3301@163.com), Z. Xing (Jmg3333@sina.com) contributed to the data analysis and part of experiment. T. Jin (garfriend@163.com), T. Liu (tingting_liu66@163.com) and Q. Xia (xiaqing@medmail.com.cn) supervised

the experiment. D.N. Criddle (criddle@liverpool.ac.uk) critically revised the manuscript. All authors read and approved the final manuscript.

Acknowledgments

The work was supported by grants from National Natural Science Foundation of China (No. 81403078, DD; No. 81703911, TJ; No. 8177141618, QX, WH, TL, TJ and DD) and the National Institute for Health Research Senior Investigator Scheme (RS). We thank Min Zhu (Standardised Laboratory Technician Training Programme) and Li Li (Pathology Laboratory) of West China Hospital for their input to this project. We also thank Dr Thompson Gana from Professor Eithne Costello's research group in the University of Liverpool for his guidance on Nrf2 antibodies and data interpretation.

Supplementary materials

Supplementary materials included one supplementary table and nine supplementary figures.

References

Anchi, P., Khurana, A., Bale, S., Godugu, C., 2017. The Role of Plant-derived Products in Pancreatitis: Experimental and Clinical Evidence. Phytother. Res. 31, 591-623.

Banks, P.A., Bollen, T.L., Dervenis, C., Gooszen, H.G., Johnson, C.D., Sarr, M.G., Tsiotos, G.G., Vege, S.S., Acute Pancreatitis Classification Working, G., 2013. Classification of acute pancreatitis--2012: revision of the Atlanta classification and definitions by international consensus. Gut. 62, 102-111.

Booth, D.M., Mukherjee, R., Sutton, R., Criddle, D.N., 2011a. Calcium and reactive oxygen species in acute pancreatitis: friend or foe? Antioxid. Redox. Signal. 15, 2683-2698.

Booth, D.M., Murphy, J.A., Mukherjee, R., Awais, M., Neoptolemos, J.P., Gerasimenko, O.V., Tepikin, A.V., Petersen, O.H., Sutton, R., Criddle, D.N., 2011b. Reactive oxygen species induced by bile acid induce apoptosis and protect against necrosis in pancreatic acinar cells. Gastroenterology. 140, 2116-2125.

Carvalho, K.M., Morais, T.C., de Melo, T.S., de Castro Brito, G.A., de Andrade, G.M., Rao, V.S., Santos, F.A., 2010. The natural flavonoid quercetin ameliorates cerulein-induced acute pancreatitis in mice. Biol. Pharm. Bull. 33, 1534-1539.

Chen, L.X., Hu, D.J., Lam, S.C., Ge, L., Wu, D., Zhao, J., Long, Z.R., Yang, W.J., Fan, B., Li, S.P., 2016. Comparison of antioxidant activities of different parts from snow chrysanthemum (Coreopsis tinctoria Nutt.) and identification of their natural antioxidants using high performance liquid chromatography coupled with diode array detection and mass spectrometry and 2,2'-azinobis(3-ethylbenzthiazoline-sulfonic acid)diammonium salt-based assay. J. Chromatogr. A. 1428, 134-142.

Cui, Y., Ran, X., 1993. Zhonghua yao hai – “The sea of Chinese Medicine”. Harbin Publishing House, 1680 pp.

Das, S.L., Singh, P.P., Phillips, A.R., Murphy, R., Windsor, J.A., Petrov, M.S., 2014. Newly diagnosed diabetes mellitus after acute pancreatitis: a systematic review and meta-analysis. Gut. 63, 818-831.

Dawra, R., Ku, Y.S., Sharif, R., Dhaulakhandi, D., Phillips, P., Dudeja, V., Saluja, A.K., 2008. An improved method for extracting myeloperoxidase and determining its activity in the pancreas and lungs during pancreatitis. Pancreas. 37, 62-68.

Dawra, R., Sah, R.P., Dudeja, V., Rishi, L., Talukdar, R., Garg, P., Saluja, A.K., 2011. Intra-acinar trypsinogen activation mediates early stages of pancreatic injury but not inflammation in mice with acute pancreatitis. Gastroenterology. 141, 2210-2217 e2212.

Dias, T., Bronze, M.R., Houghton, P.J., Mota-Filipe, H., Paulo, A., 2010. The flavonoid-rich fraction of Coreopsis tinctoria promotes glucose tolerance

regain through pancreatic function recovery in streptozotocin-induced glucose-intolerant rats. J. Ethnopharmacol. 132, 483-490.
Dias, T., Liu, B., Jones, P., Houghton, P.J., Mota-Filipe, H., Paulo, A., 2012. Cytoprotective effect of Coreopsis tinctoria extracts and flavonoids on tBHP and cytokine-induced cell injury in pancreatic MIN6 cells. J. Ethnopharmacol. 139, 485-492.
D'Oliveira Feijão, R., 1973. Medicina pelas plantas, sixth ed. Livraria Progresso Editora, Lisboa, pp. 19, 156.
Dong, Z., Shang, H., Chen, Y.Q., Pan, L.L., Bhatia, M., Sun, J., 2016. Sulforaphane Protects Pancreatic Acinar Cell Injury by Modulating Nrf2-Mediated Oxidative Stress and NLRP3 Inflammatory Pathway. Oxid. Med. Cell. Longev. 2016, 7864150.
Du, D., Jin, T., Xing, Z.H., Hu, L.Q., Long, D., Li, S.F., Gong, M., 2016. One new linear C14 polyacetylene glucoside with antiadipogenic activities on 3T3-L1 cells from the capitula of Coreopsis tinctoria. J. Asian. Nat. Prod. Res. 18, 784-790.
Forsmark, C.E., Vege, S.S., and Wilcox, C.M., 2016. Acute Pancreatitis. N. Engl. J. Med. 375, 1972-1981.
Foster, S., Duke, J.A., 1990. A Field Guide to Medicinal Plants. Eastern and Central North America. Houghton Mifflin Co.
Guo, J., Wang, A., Yang, K., Ding, H., Hu, Y., Yang, Y., Huang, S., Xu, J., Liu, T., Yang, H., et al., 2017. Isolation, characterization and antimicrobial activities of polyacetylene glycosides from Coreopsis tinctoria Nutt. Phytochemistry. 136, 65-69.
Hackert, T., and Werner, J., 2011. Antioxidant therapy in acute pancreatitis: experimental and clinical evidence. Antioxid. Redox. Signal. 15, 2767-2777.
Hu, Q., Zhang, D.D., Wang, L., Lou, H., Ren, D., 2012. Eriodictyol-7-O-glucoside, a novel Nrf2 activator, confers protection against cisplatin-induced toxicity. Food. Chem. Toxicol. 50, 1927-1932.
Huang, W., Booth, D.M., Cane, M.C., Chvanov, M., Javed, M.A., Elliott, V.L., Armstrong, J.A., Dingsdale, H., Cash, N., Li, Y., et al., 2014. Fatty acid ethyl ester synthase inhibition ameliorates ethanol-induced Ca2+-dependent mitochondrial dysfunction and acute pancreatitis. Gut. 63, 1313-1324.
Huang, W., Cane, M.C., Mukherjee, R., Szatmary, P., Zhang, X., Elliott, V., Ouyang, Y., Chvanov, M., Latawiec, D., Wen, L., et al., 2017a. Caffeine protects against experimental acute pancreatitis by inhibition of inositol 1,4,5-trisphosphate receptor-mediated Ca2+ release. Gut. 66, 301-313.
Huang, W., Haynes, A.C., Mukherjee, R., Wen, L., Latawiec, D., Tepikin, A.V., Criddle, D.N., Prinjha, R.K., Smithers, N., Sutton, R., 2017b. Selective inhibition of BET proteins reduces pancreatic damage and systemic inflammation in bile acid- and fatty acid ethyl ester- but not caerulein-induced acute pancreatitis. Pancreatology. 17, 689-697.

Huang, W., Szatmary, P., Wan, M., Bharucha, S., Awais, M., Tang, W., Criddle, D.N., Xia, Q., Sutton, R., 2016. Translational Insights Into Peroxisome Proliferator-Activated Receptors in Experimental Acute Pancreatitis. Pancreas. 45, 167-178.

Hybertson, B.M., Gao, B., Bose, S.K., McCord, J.M., 2011. Oxidative stress in health and disease: the therapeutic potential of Nrf2 activation. Mol. Aspects. Med. 32, 234-246.

Jiang, B., Le, L., Wan, W., Zhai, W., Hu, K., Xu, L., Xiao, P., 2015. The Flower Tea Coreopsis tinctoria Increases Insulin Sensitivity and Regulates Hepatic Metabolism in Rats Fed a High-Fat Diet. Endocrinology. 156, 2006-2018.

Johansen, J.S., Harris, A.K., Rychly, D.J., Ergul, A., 2005. Oxidative stress and the use of antioxidants in diabetes: linking basic science to clinical practice. Cardiovasc. Diabetol. 4, 5.

Jung, K.H., Hong, S.W., Zheng, H.M., Lee, H.S., Lee, H., Lee, D.H., Lee, S.Y., Hong, S.S., 2010. Melatonin ameliorates cerulein-induced pancreatitis by the modulation of nuclear erythroid 2-related factor 2 and nuclear factor-kappaB in rats. J. Pineal. Res. 48, 239-250.

Khaled, K.A., El-Sayed, Y.M., and Al-Hadiya, B.M., 2003. Disposition of the flavonoid quercetin in rats after single intravenous and oral doses. Drug. Dev. Ind. Pharm. 29, 397-403.

Lerch, M.M., and Gorelick, F.S., 2013. Models of acute and chronic pancreatitis. Gastroenterology. 144, 1180-1193.

Leung, P.S., and Chan, Y.C., 2009. Role of oxidative stress in pancreatic inflammation. Antioxid. Redox. Signal. 11, 135-165.

Ma, Q., 2013. Role of nrf2 in oxidative stress and toxicity. Annu. Rev. Pharmacol. Toxicol. 53, 401-426.

Magesh, S., Chen, Y., and Hu, L., 2012. Small molecule modulators of Keap1-Nrf2-ARE pathway as potential preventive and therapeutic agents. Med. Res. Rev. 32, 687-726.

Mankad, P., James, A., Siriwardena, A.K., Elliott, A.C., Bruce, J.I., 2012. Insulin protects pancreatic acinar cells from cytosolic calcium overload and inhibition of plasma membrane calcium pump. J. Biol. Chem. 287, 1823-1836.

Maritim, A.C., Sanders, R.A., and Watkins, J.B., 2003. Diabetes, oxidative stress, and antioxidants: a review. J. Biochem. Mol. Toxicol. 17, 24-38.

Moggia, E., Koti, R., Belgaumkar, A.P., Fazio, F., Pereira, S.P., Davidson, B.R., Gurusamy, K.S., 2017. Pharmacological interventions for acute pancreatitis. Cochrane. Database. Syst. Rev. 4, CD011384.

Mukherjee, R., Mareninova, O.A., Odinokova, I.V., Huang, W., Murphy, J., Chvanov, M., Javed, M.A., Wen, L., Booth, D.M., Cane, M.C., et al., 2016. Mechanism of mitochondrial permeability transition pore induction and damage in the pancreas: inhibition prevents acute pancreatitis by protecting production of ATP. Gut. 65, 1333-1346.

Peery, A.F., Crockett, S.D., Barritt, A.S., Dellon, E.S., Eluri, S., Gangarosa, L.M., Jensen, E.T., Lund, J.L., Pasricha, S., Runge, T., et al., 2015. Burden of Gastrointestinal, Liver, and Pancreatic Diseases in the United States. Gastroenterology. 149, 1731-1741 e1733.

Perides, G., van Acker, G.J., Laukkarinen, J.M., and Steer, M.L., 2010. Experimental acute biliary pancreatitis induced by retrograde infusion of bile acids into the mouse pancreatic duct. Nat. Protoc. 5, 335-341.

Robles, L., Vaziri, N.D., Li, S., Masuda, Y., Takasu, C., Takasu, M., Vo, K., Farzaneh, S.H., Stamos, M.J., Ichii, H., 2016. Synthetic Triterpenoid RTA dh404 (CDDO-dhTFEA) Ameliorates Acute Pancreatitis. Pancreas. 45, 720-729.

Saluja, A.K., Lerch, M.M., Phillips, P.A., Dudeja, V., 2007. Why does pancreatic overstimulation cause pancreatitis? Annu. Rev. Physiol. 69, 249-269.

Samad, A., James, A., Wong, J., Mankad, P., Whitehouse, J., Patel, W., Alves-Simoes, M., Siriwardena, A.K., Bruce, J.I., 2014. Insulin protects pancreatic acinar cells from palmitoleic acid-induced cellular injury. J. Biol. Chem. 289, 23582-23595.

Shapiro, H., Singer, P., Halpern, Z., Bruck, R., 2007. Polyphenols in the treatment of inflammatory bowel disease and acute pancreatitis. Gut. 56, 426-435.

Tsai, J.C., Chiu, C.S., Chen, Y.C., Lee, M.S., Hao, X.Y., Hsieh, M.T., Kao, C.P., Peng, W.H., 2017. Hepatoprotective effect of Coreopsis tinctoria flowers against carbon tetrachloride-induced liver damage in mice. BMC Complement. Altern. Med. 17, 139.

van Dijk, S.M., Hallensleben, N.D.L., van Santvoort, H.C., Fockens, P., van Goor, H., Bruno, M.J., Besselink, M.G., Dutch Pancreatitis Study, G., 2017. Acute pancreatitis: recent advances through randomised trials. Gut. 66, 2024-2032.

Wan, M.H., Huang, W., Latawiec, D., Jiang, K., Booth, D.M., Elliott, V., Mukherjee, R., Xia, Q., 2012. Review of experimental animal models of biliary acute pancreatitis and recent advances in basic research. HPB (Oxford). 14, 73-81.

Wang, T., Xi, M., Guo, Q., Wang, L., Shen, Z., 2015. Chemical components and antioxidant activity of volatile oil of a Compositae tea (Coreopsis tinctoria Nutt.) from Mt. Kunlun. Ind. Crop. Prod. 67, 318-323.

Wang, Y.Z., Zhang, Y.C., Cheng, J.S., Ni, Q., Li, P.W., Han, W., Zhang, Y.L., 2014. Protective effects of BML-111 on cerulein-induced acute pancreatitis-associated lung injury via activation of Nrf2/ARE signaling pathway. Inflammation. 37, 1120-1133.

Wen, L., Voronina, S., Javed, M.A., Awais, M., Szatmary, P., Latawiec, D., Chvanov, M., Collier, D., Huang, W., Barrett, J., et al., 2015. Inhibitors of ORAI1 Prevent Cytosolic Calcium-Associated Injury of Human Pancreatic Acinar Cells and Acute Pancreatitis in 3 Mouse Models. Gastroenterology. 149, 481-492 e487.

Wildi, S., Kleeff, J., Mayerle, J., Zimmermann, A., Bottinger, E.P., Wakefield, L., Buchler, M.W., Friess, H., Korc, M., 2007. Suppression of transforming growth factor beta signalling aborts caerulein induced pancreatitis and eliminates restricted stimulation at high caerulein concentrations. Gut. 56, 685-692.

Xiao, A.Y., Tan, M.L., Wu, L.M., Asrani, V.M., Windsor, J.A., Yadav, D., Petrov, M.S., 2016. Global incidence and mortality of pancreatic diseases: a systematic review, meta-analysis, and meta-regression of population-based cohort studies. Lancet. Gastroenterol. Hepatol. 1, 45-55.

Yang, L.L., Xiao, N., Li, X.W., Fan, Y., Alolga, R.N., Sun, X.Y., Wang, S.L., Li, P., Qi, L.W., 2016. Pharmacokinetic comparison between quercetin and quercetin 3-O-beta-glucuronide in rats by UHPLC-MS/MS. Sci. Rep. 6, 35460.

Yu, Q.H., Zhang, P.X., Liu, Y., Liu, W., Yin, N., 2016. Hyperbaric oxygen preconditioning protects the lung against acute pancreatitis induced injury via attenuating inflammation and oxidative stress in a nitric oxide dependent manner. Biochem. Biophys. Res. Commun. 478, 93-100.

Zhang, R., Wen, L., Shen, Y., Shi, N., Xing, Z., Xia, Q., Niu, H., Huang, W., 2016. One compound of saponins from Disocorea zingiberensis protected against experimental acute pancreatitis by preventing mitochondria-mediated necrosis. Sci. Rep. 6, 35965.

Zheng, J., Wu, J., Chen, J., Liu, J., Lu, Y., Huang, C., Hu, G., Wang, X., Zeng, Y., 2016. Therapeutic effects of quercetin on early inflammation in hypertriglyceridemia-related acute pancreatitis and its mechanism. Pancreatology. 16, 200-210.

Zhou, X., and Xue, C., 2009. Ghrelin inhibits the development of acute pancreatitis and nuclear factor kappaB activation in pancreas and liver. Pancreas. 38, 752-757.

Supporting Information

Supplementary tables

Table S-1. Flavonoids identified from the total flavonoids extract based on its LC-MS BPI chromatography (Page 52)

Supplementary figures

Figure S-1. Procedure of isolating total flavonoid extract and compounds **1**-**6**. TE, total extract; CP, components of *C. tinctoria* after first isolation using polyamide; TFE, total flavonoids extract. (Page 53)

Figure S-2. ^{1}H and ^{13}C NMR Spectra of Compound **1.** (Page 54)

Figure S-3. ^{1}H and ^{13}C NMR Spectra of Compound **2.** (Page 55)

Figure S-4. ^{1}H and ^{13}C NMR Spectra of Compound **3.** (Page 56)

Figure S-5. ^{1}H and ^{13}C NMR Spectra of Compound **4.** (Page 57)

Figure S-6. ^{1}H and ^{13}C NMR Spectra of Compound **5.** (Page 58)

Figure S-7. ^{1}H and ^{13}C NMR Spectra of Compound **6.** (Page 59)

Figure S-8. Effects of total extract (TE) and components of *C. tinctoria* after first isolation using polyamide (CP) on necrotic cell death activation in mouse pancreatic acinar cells. Cells were treated with normal saline or taurocholic acid sodium salt hydrate (NaT, 5 mM) with or without extractions at designated concentrations. The necrosis % (PI uptake) induced by NaT was calculated from Hoechst 33342 stained cells and multiply by 100 %. Effects of TE and CP were assessed at the concentration of 1 mM. Data are expressed as mean ± SEM from 3 or more independent experiments. $^{*}P < 0.05$ vs. model group, $^{\#}P$

< 0.001 vs. control group. In the histogram: *dark grey* = control, *black* = NaT, and *white* = NaT with TE or CP. (Page 60)

Figure S-9. Effects of C**1** on severity of bile acid-induced acute pancreatitis (TLCS-AP) in mice. TLCS-AP was induced by retrograde infusion of 3.5% taurolithocholic acid 3-sulfate disodium salt into the pancreatic duct, while control mice received sham operation. In the treatment group, rats received intraperitoneal injections of C**1** (12.5 mg/kg) at 0, 4 and 8 hours post-operation. All mice were sacrificed at 24 hours post-operation. (A) C**1** reduced pancreatic histopathology damage: (i) representative haematoxylin and eosin (H&E) sections of pancreas from control, TLCS, and TLCS with C**1**. (ii) overall histopathology score and its breakdown scores - (iii) oedema, (iv) inflammation and (v) necrosis. (B) Serum amylase. (C) Serum lipase. Data are expressed as means ± SEM from 5 or more animals per each group. **P* < 0.05 vs. TLCS group, $^{\#}P$ < 0.001 vs. control group. In the histogram: *dark grey* = control, *black* = TLCS, and *white* = TLCS with C**1**. (Page 61)

Table S-1 Flavonoids identified from the total flavonoids extract based on its LC-MS BPI chromatography

NO.	Component name	Formula	RT	Observed m/z	Mass error (mDa)	Detector counts	Adducts
1	Dihydroquercetin 7-O-glucoside	$C_{21}H_{22}O_{12}$	3.22	465.1031	-0.71	341995	-H
2	Dihydroquercetin 7-O-glucoside	$C_{21}H_{22}O_{12}$	3.48	465.1026	-1.23	40018	-H
3	Flavanomarein	$C_{21}H_{22}O_{11}$	3.93	449.1076	-1.31	2119268	-H
4	6-hydroxy kaempferol 7-O-glucoside	$C_{21}H_{20}O_{12}$	4.12	463.0870	-1.15	76063	-H
5	4',5,7-trihydroxy-flavone 3-O-glucoside	$C_{21}H_{22}O_{10}$	4.14	433.1128	-1.26	345186	-H
6	Quercetagetin 7-O-glucoside	$C_{21}H_{20}O_{13}$	4.28	479.0815	-1.65	1190623	-H, +HCOO
7	3,5,7,4'-tetrahydroxy flavanone	$C_{15}H_{12}O_6$	4.68	287.0556	-0.56	837951	-H
8	Marein isomer	$C_{21}H_{22}O_{11}$	4.80	449.1079	-1.08	1072511	-H
9	Maritimein	$C_{21}H_{20}O_{11}$	4.80	447.0925	-0.81	726802	-H, +HCOO
10	Hyperin	$C_{21}H_{20}O_{12}$	4.85	463.0875	-0.71	365908	-H
11	Marein	$C_{21}H_{22}O_{11}$	4.90	449.1078	-1.18	3891522	-H
12	Luteolin 7-O-glucoside	$C_{21}H_{20}O_{11}$	4.95	447.0923	-0.94	117442	-H
13	Marigold glucoside	$C_{22}H_{22}O_{13}$	5.00	493.0974	-1.40	156799	-H, +HCOO
14	7-O-glucosyl-kaempferol	$C_{21}H_{20}O_{11}$	5.43	447.0922	-1.06	38977	-H
15	Coreopsin	$C_{21}H_{22}O_{10}$	5.52	433.1128	-1.25	1539334	-H
16	8-hydroxy fustin	$C_{15}H_{12}O_6$	5.97	287.0553	-0.79	531429	-H
17	Okanin	$C_{15}H_{12}O_6$	6.49	287.0546	-1.49	20769	-H
18	Quercetin	$C_{15}H_{10}O_7$	6.69	301.0345	-0.92	38318	-H
19	7,3',5'-trihydroxy flavanone	$C_{15}H_{12}O_5$	7.32	271.0602	-0.99	28096	-H

Figure S-1.

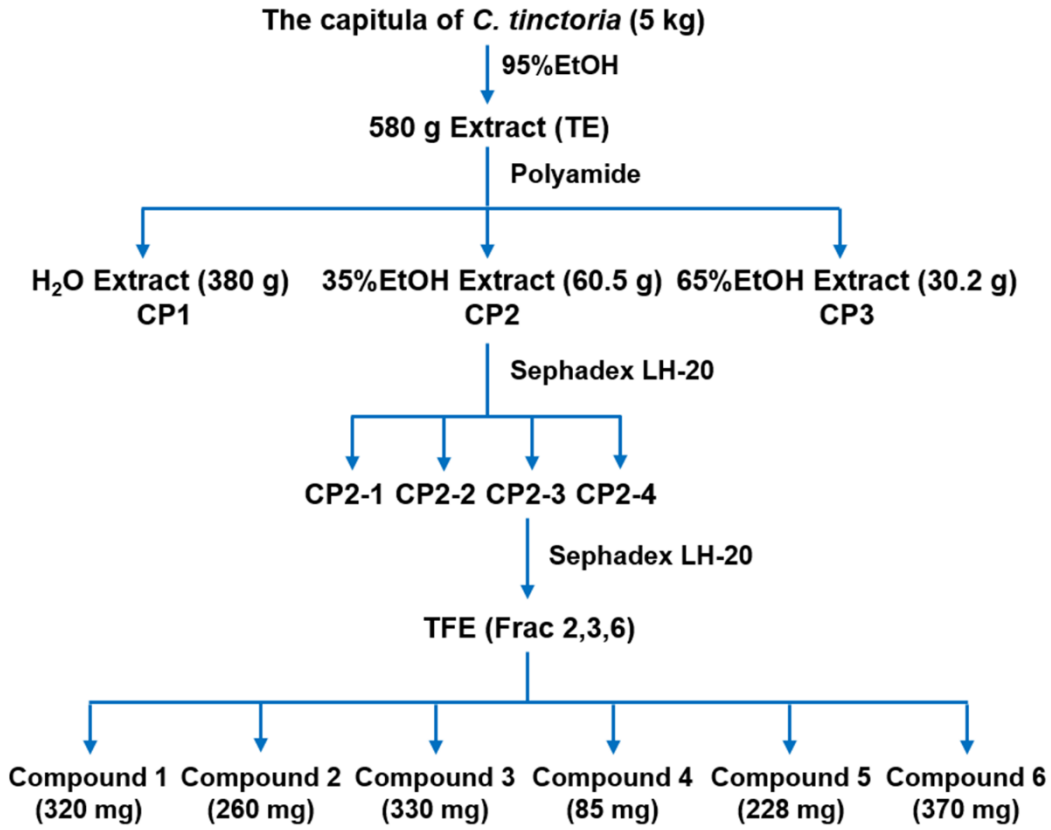
The capitula of C. tinctoria (5 kg)
95%EtOH
580 g Extract (TE)
Polyamide
H2O Extract (380 g)
CP1
35%EtOH Extract (60.5 g)
CP2
65%EtOH Extract (30.2 g)
CP3
Sephadex LH-20
CP2-1 CP2-2 CP2-3 CP2-4
Sephadex LH-20
TFE (Frac 2,3,6)
Compound 1 (320 mg)
Compound 2 (260 mg)
Compound 3 (330 mg)
Compound 4 (85 mg)
Compound 5 (228 mg)
Compound 6 (370 mg)

Figure S-2.

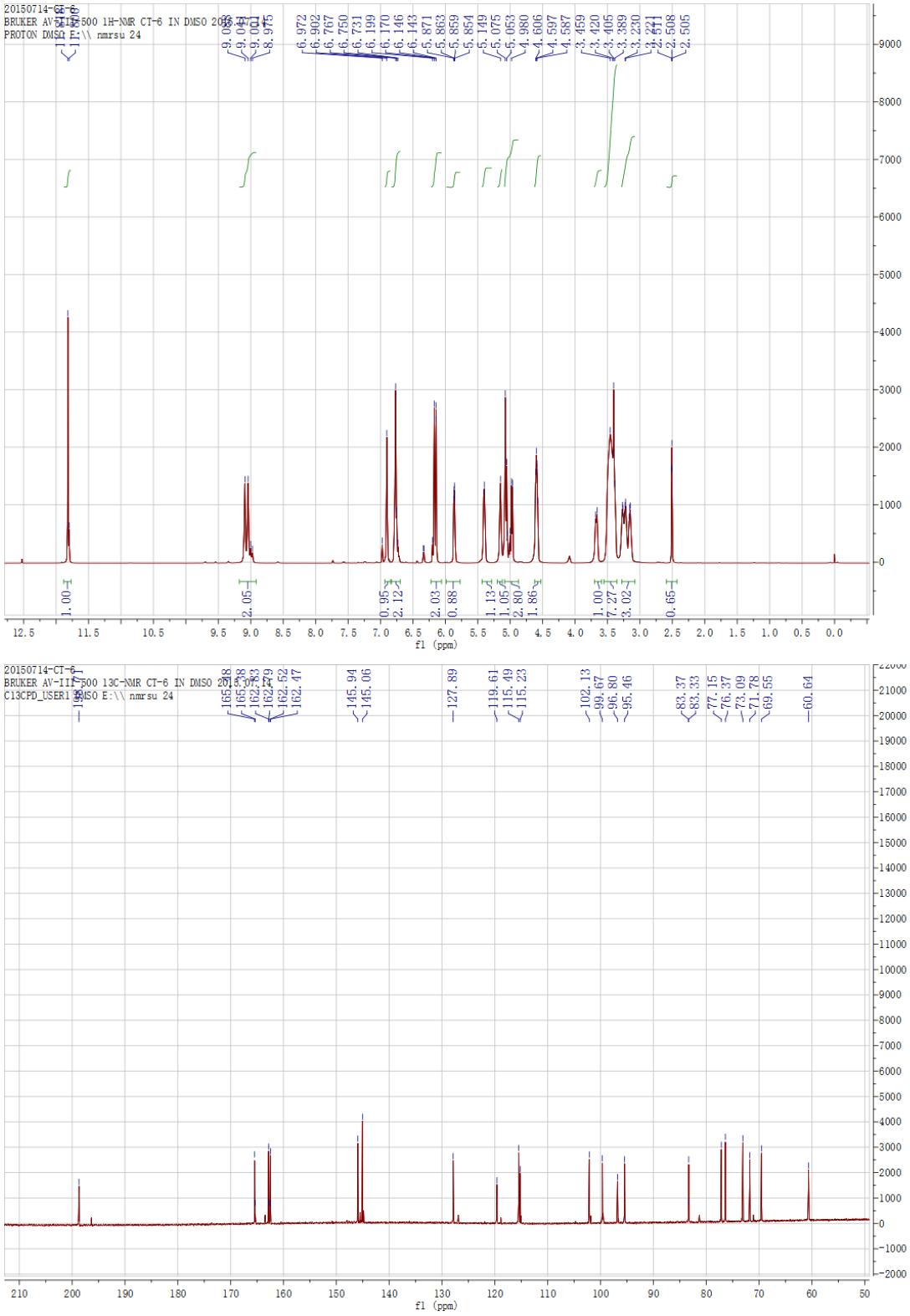

Figure S-3.

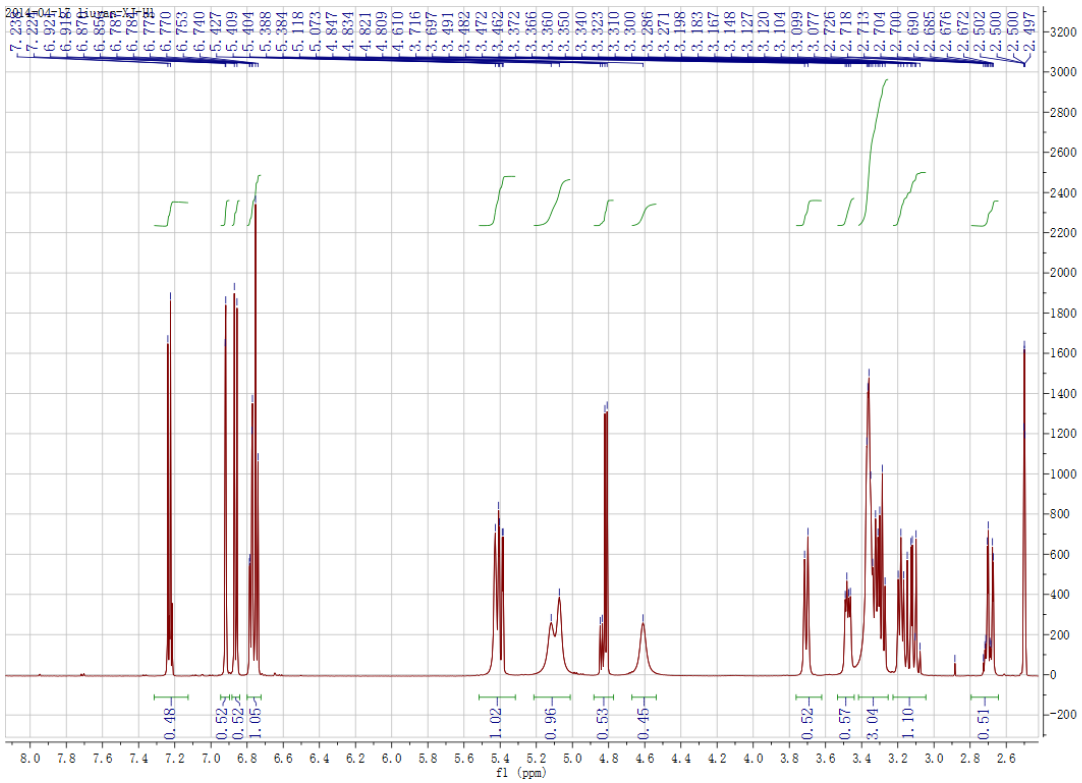

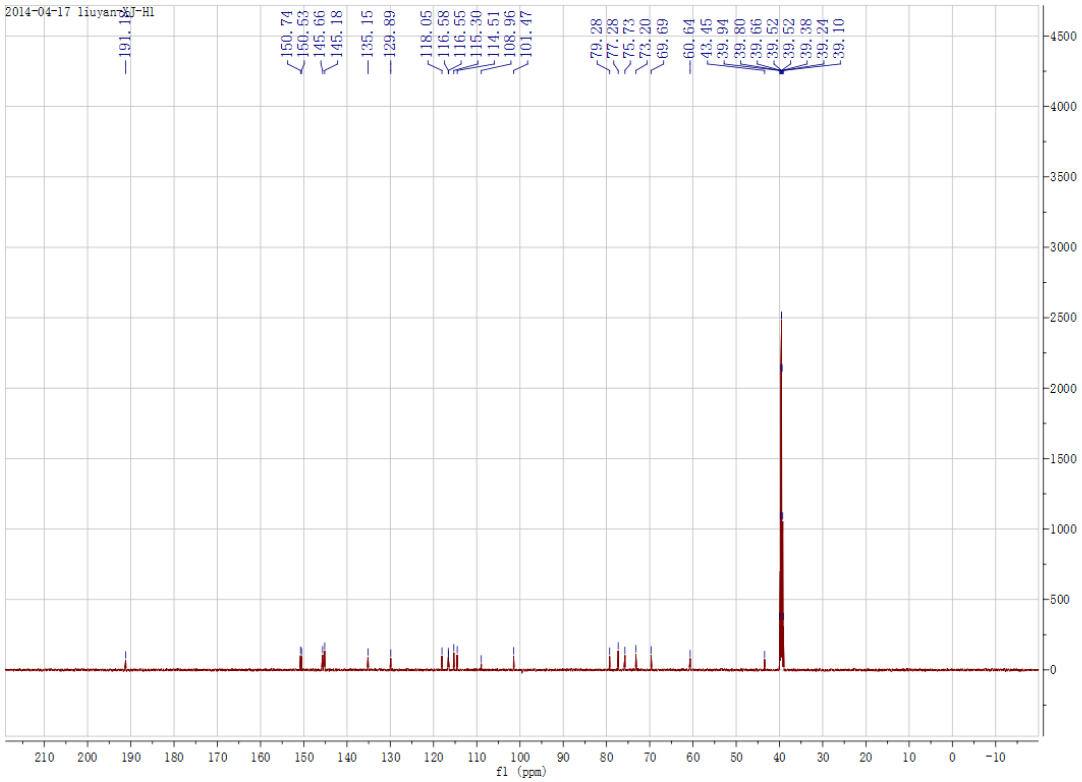

Figure S-4.

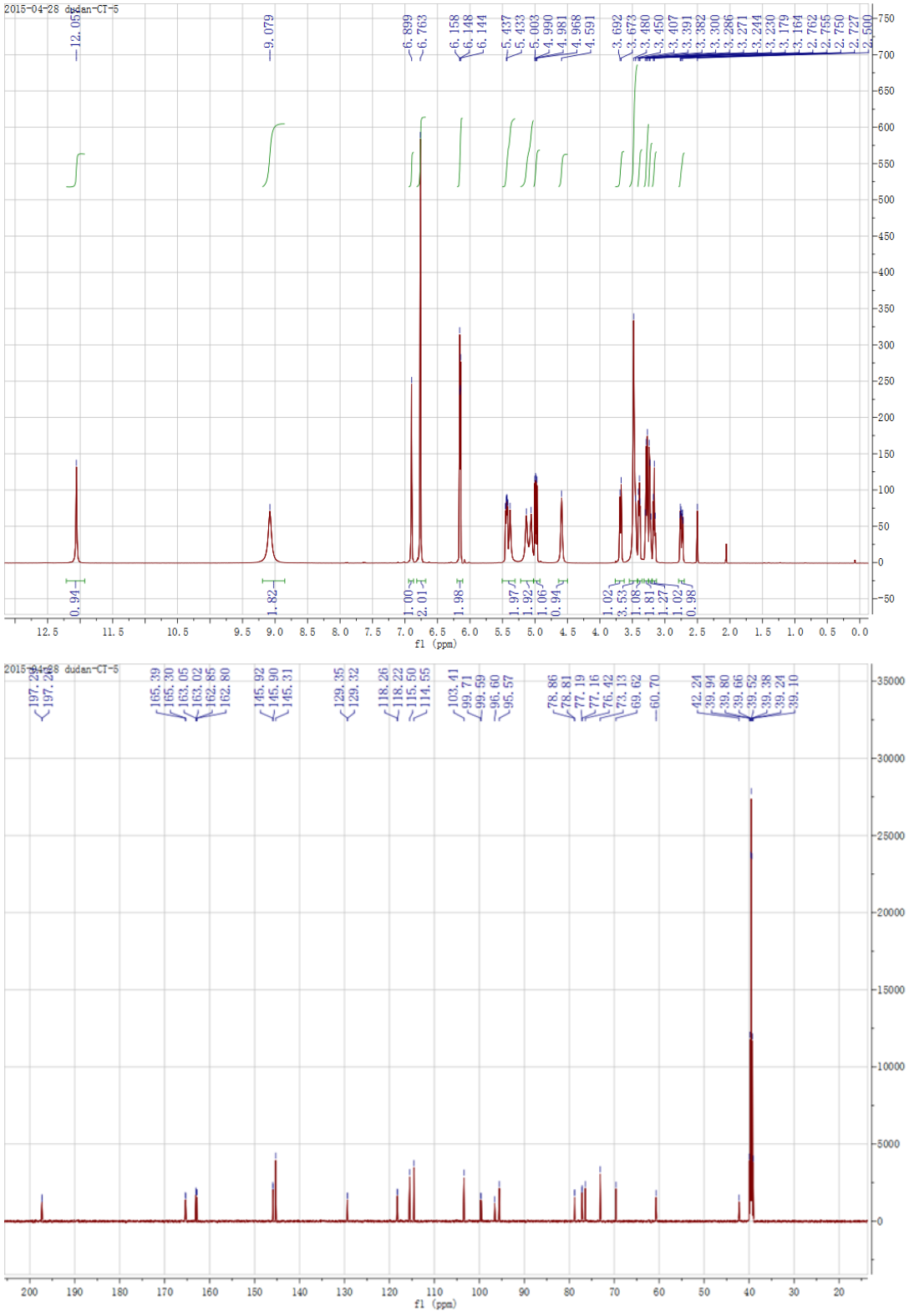

Figure S-5.

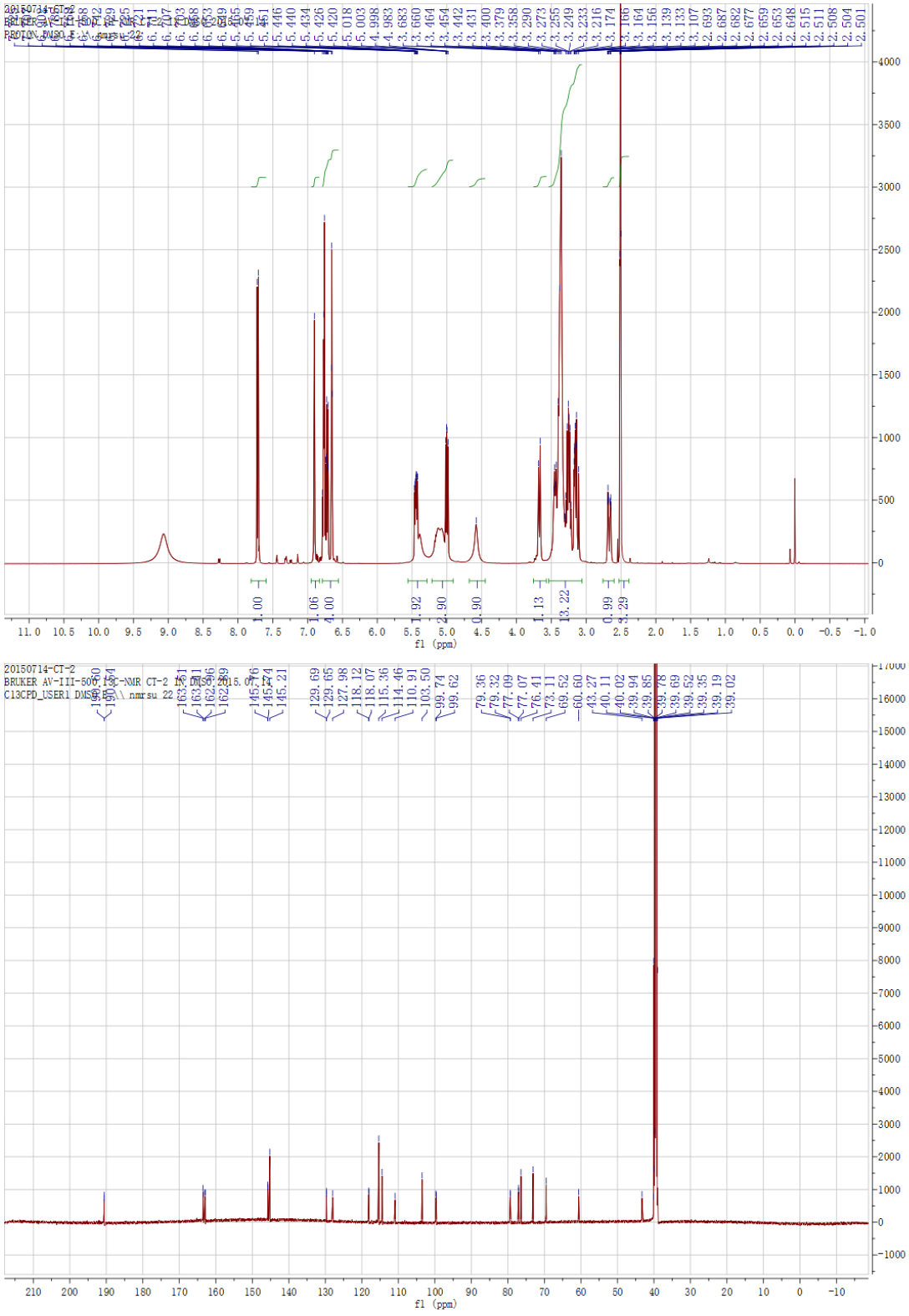

Figure S-6.

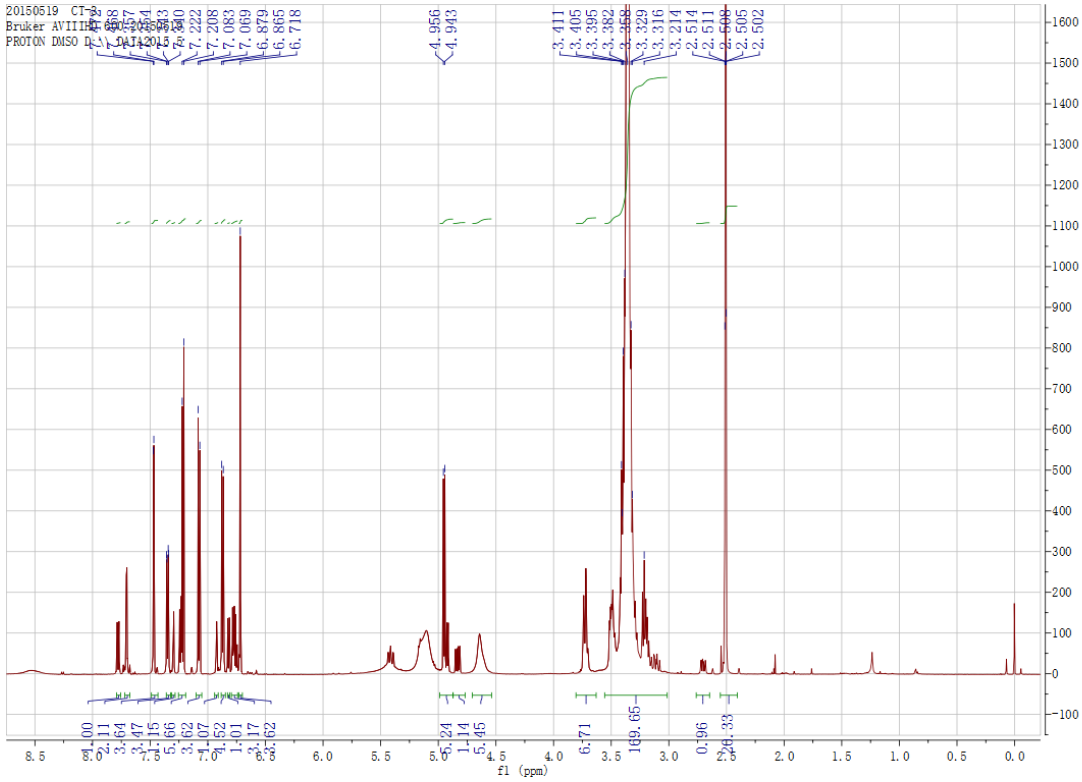
20150519 CT-3
Bruker AVIIIHD 600 20150519
PROTON DMSO D:\\ DATA2015 5
f1 (ppm)

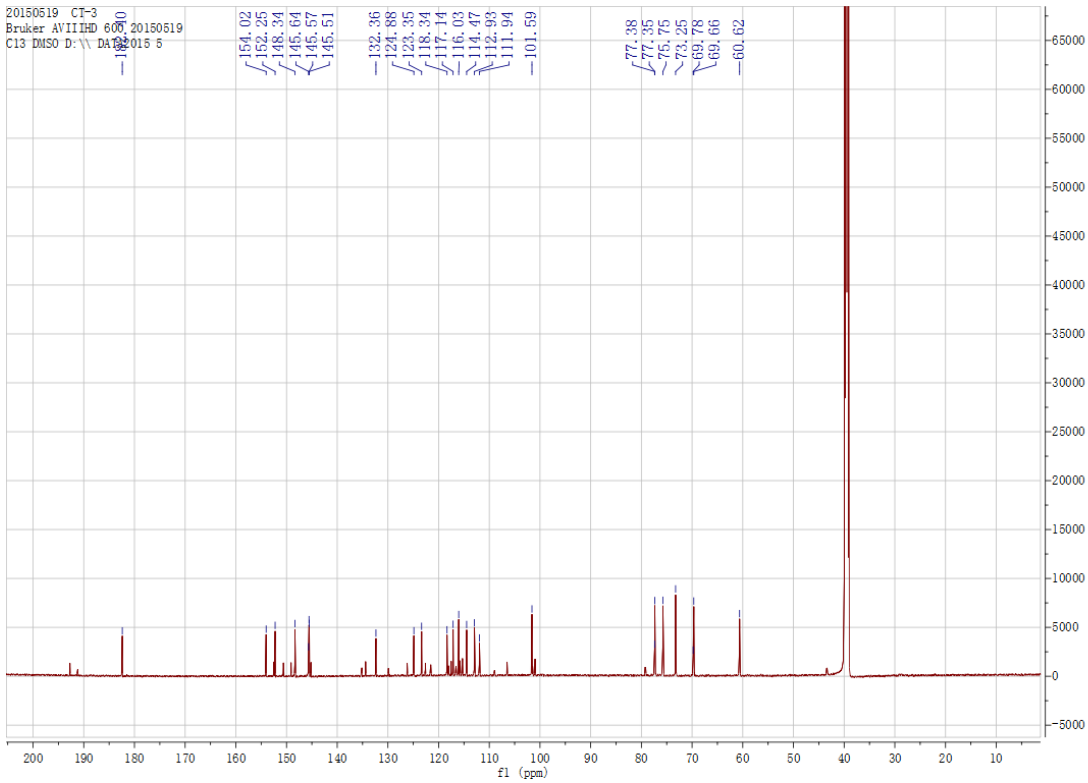
20150519 CT-3
Bruker AVIIIHD 600 20150519
C13 DMSO D:\\ DATA2015 5
f1 (ppm)

Figure S-7.

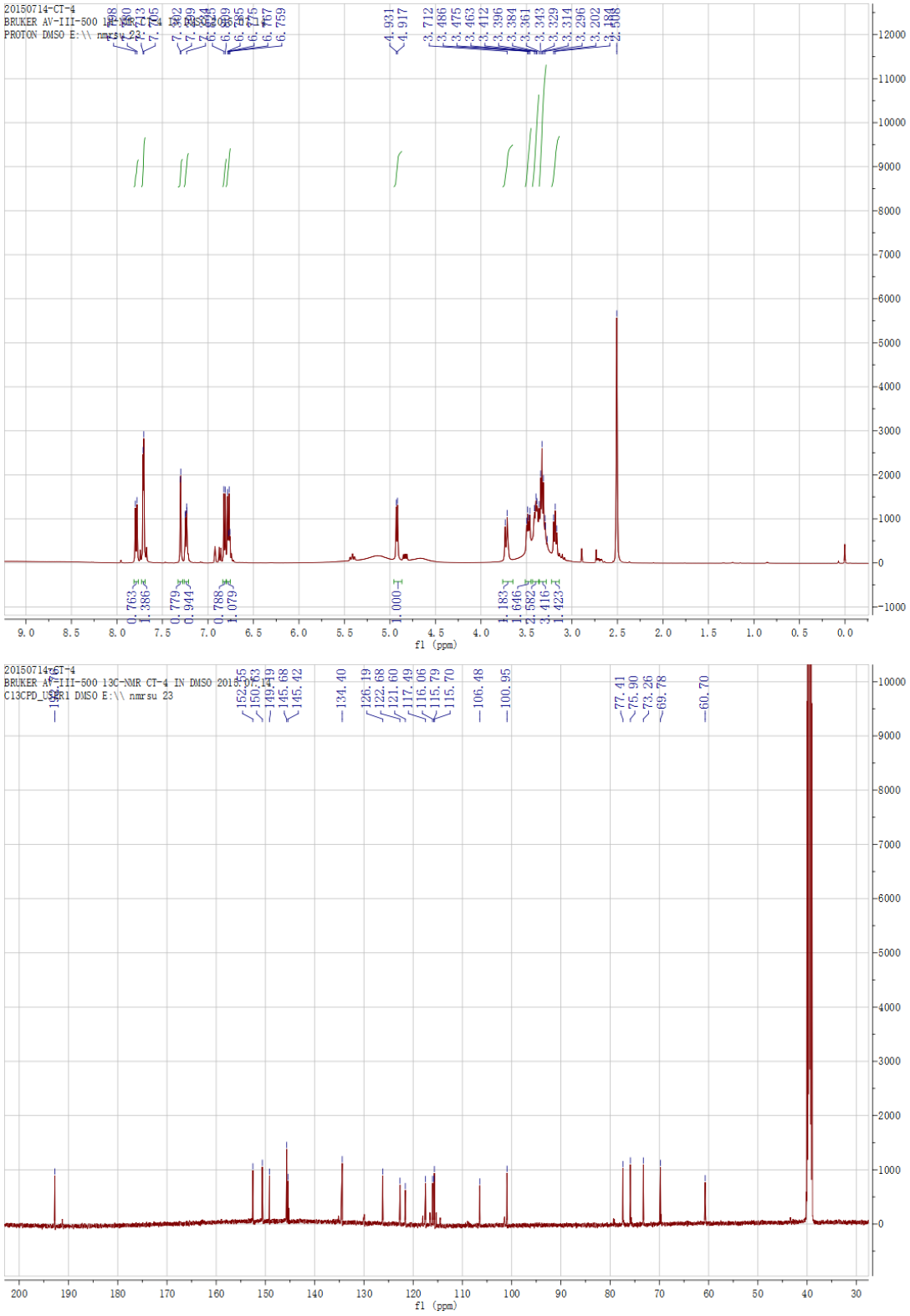
20150714-CT-4
PROTON DMSO E:\\ nmrsu 23
f1 (ppm)
20150714-CT-4
C13CPD_USER1 DMSO E:\\ nmrsu 23
f1 (ppm)

Figure S-8.

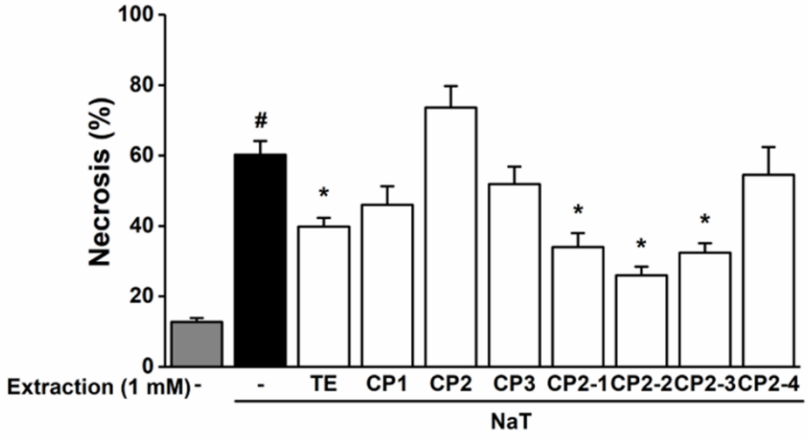
Necrosis (%)
100
80
60
40
20
0
#
*
*
*
*
Extraction (1 mM) -
-
TE
CP1
CP2
CP3
CP2-1
CP2-2
CP2-3
CP2-4
NaT

Figure S-9.

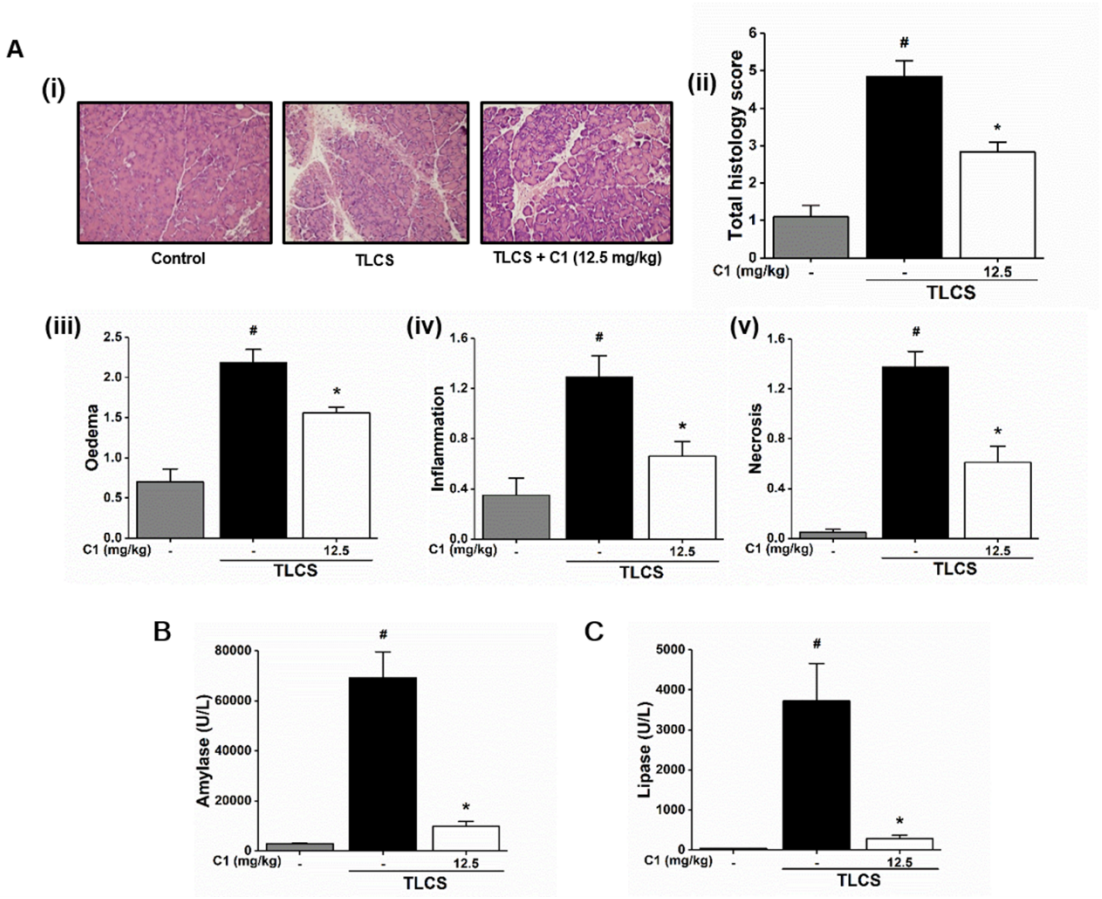
A
(i)
Control
TLCS
TLCS + C1 (12.5 mg/kg)
(ii)
Total histology score
C1 (mg/kg)
TLCS
(iii)
Oedema
(iv)
Inflammation
(v)
Necrosis
B
Amylase (U/L)
C
Lipase (U/L)

A

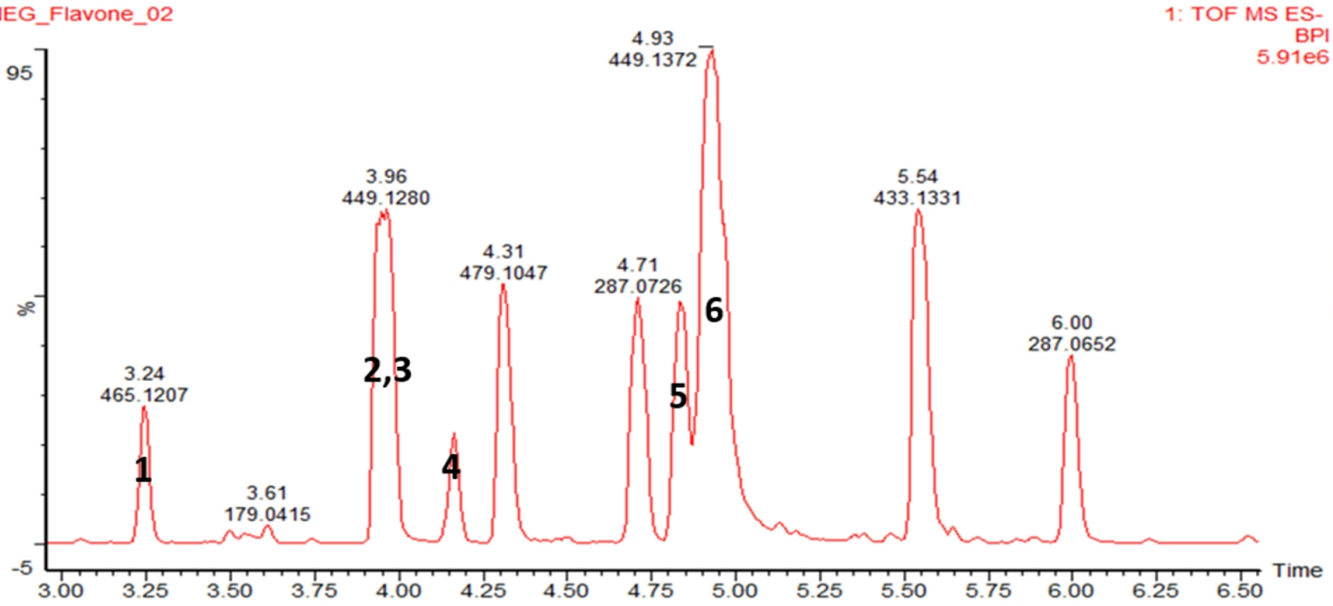
NEG_Flavone_02
1: TOF MS ES-
BPI
5.91e6
95
%
-5
3.24
465.1207
3.61
179.0415
3.96
449.1280
4.31
479.1047
4.71
287.0726
4.93
449.1372
5.54
433.1331
6.00
287.0652
1
2,3
4
5
6
Time
3.00
3.25
3.50
3.75
4.00
4.25
4.50
4.75
5.00
5.25
5.50
5.75
6.00
6.25
6.50

B

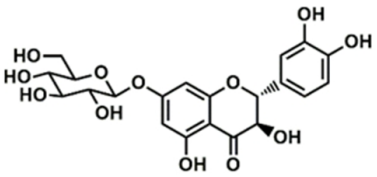
HO
HO
HO
OH
O
OH
OH
OH
OH
O

1

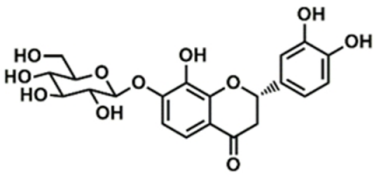
HO
HO
HO
OH
O
OH
OH
OH
OH
O

2

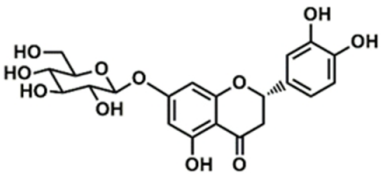
HO
HO
HO
OH
O
OH
OH
OH
OH
O

3

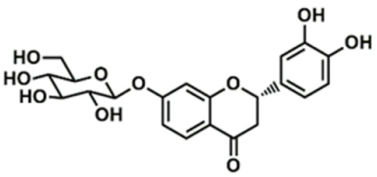
HO
HO
HO
OH
O
OH
OH
OH
O

4

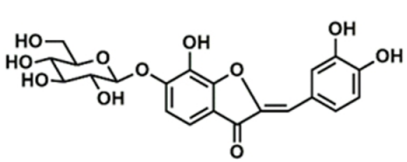
HO
HO
HO
OH
O
OH
OH
OH
O

5

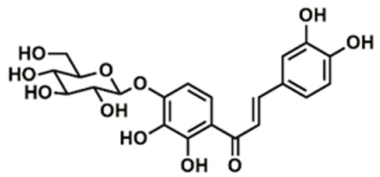
HO
HO
HO
OH
HO
OH
OH
OH
O

6

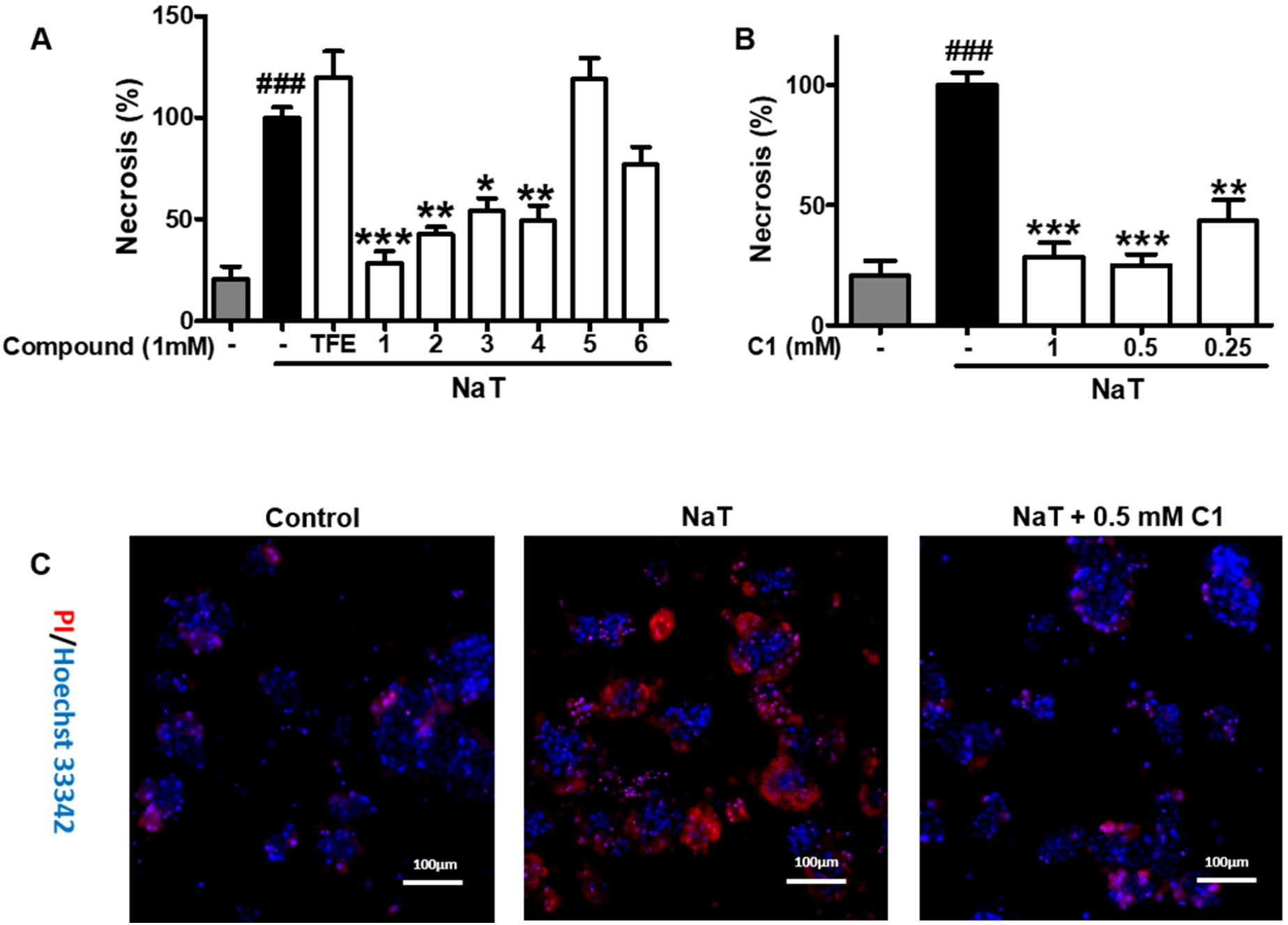
A
Necrosis (%)
150
100
50
0
###
***
**
*
**
Compound (1mM) - - TFE 1 2 3 4 5 6
NaT
B
Necrosis (%)
100
50
0
###
***
***
**
C1 (mM) - - 1 0.5 0.25
NaT
C
PI/Hoechst 33342
Control
NaT
NaT + 0.5 mM C1
100μm
100μm
100μm

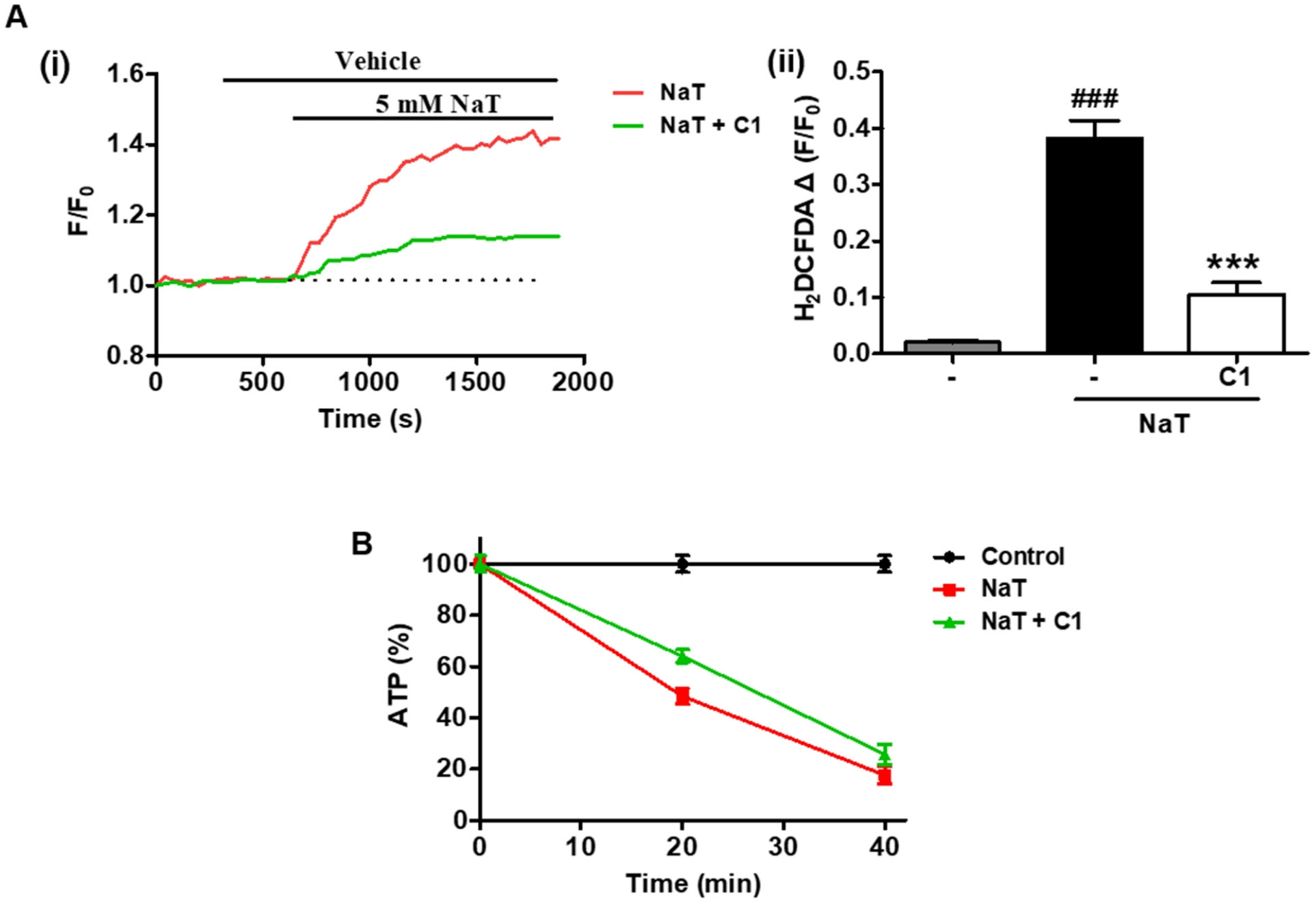
A
(i)
Vehicle
5 mM NaT
NaT
NaT + C1
F/F0
1.6
1.4
1.2
1.0
0.8
0
500
1000
1500
2000
Time (s)
(ii)
H2DCFDA Δ (F/F0)
0.5
0.4
0.3
0.2
0.1
0.0
###
***
-
-
C1
NaT
B
ATP (%)
100
80
60
40
20
0
0
10
20
30
40
Time (min)
Control
NaT
NaT + C1

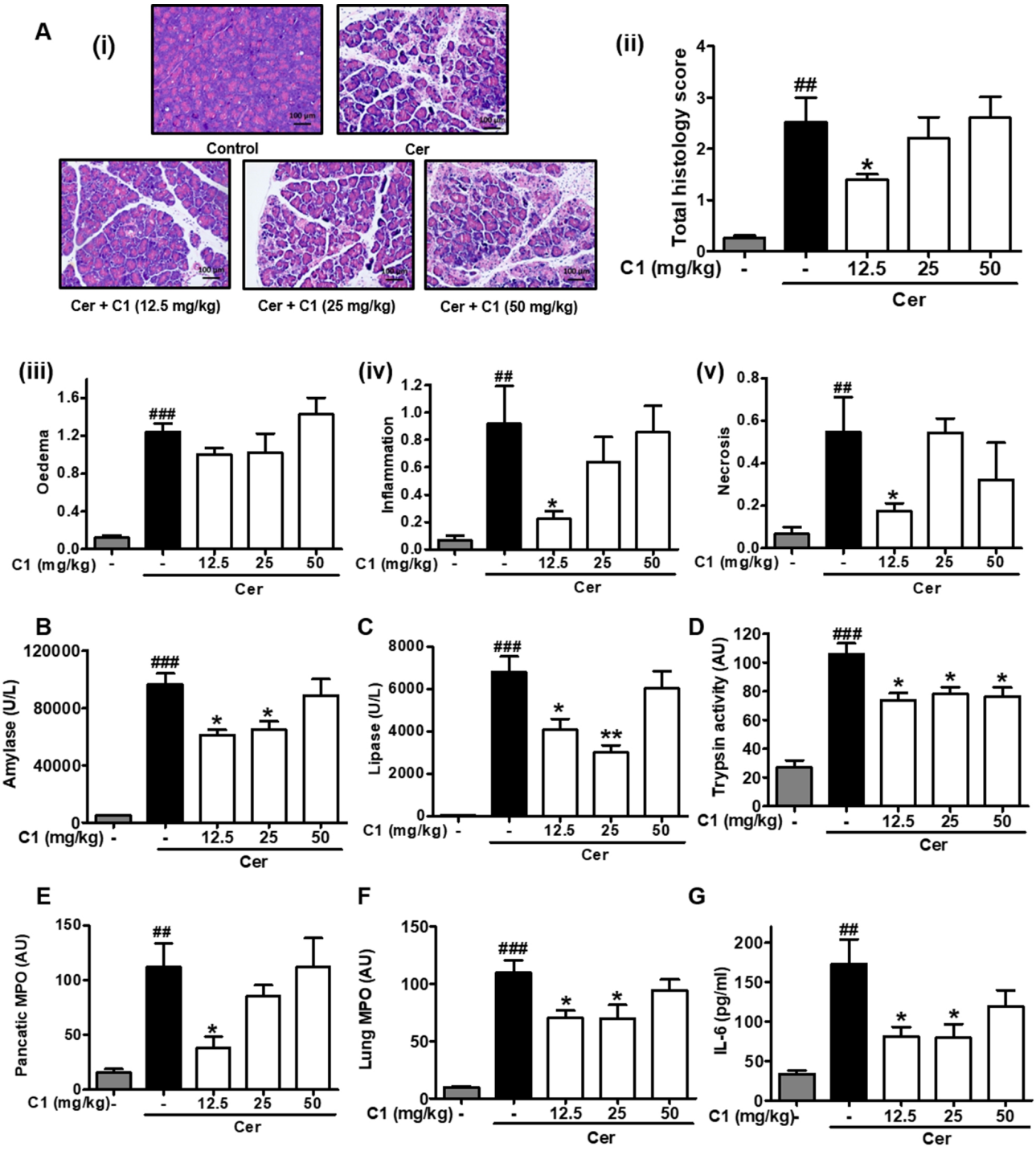
A
(i)
Control
Cer
Cer + C1 (12.5 mg/kg)
Cer + C1 (25 mg/kg)
Cer + C1 (50 mg/kg)
(ii)
Total histology score
C1 (mg/kg)
Cer
(iii)
Oedema
(iv)
Inflammation
(v)
Necrosis
B
Amylase (U/L)
C
Lipase (U/L)
D
Trypsin activity (AU)
E
Pancatic MPO (AU)
F
Lung MPO (AU)
G
IL-6 (pg/ml)

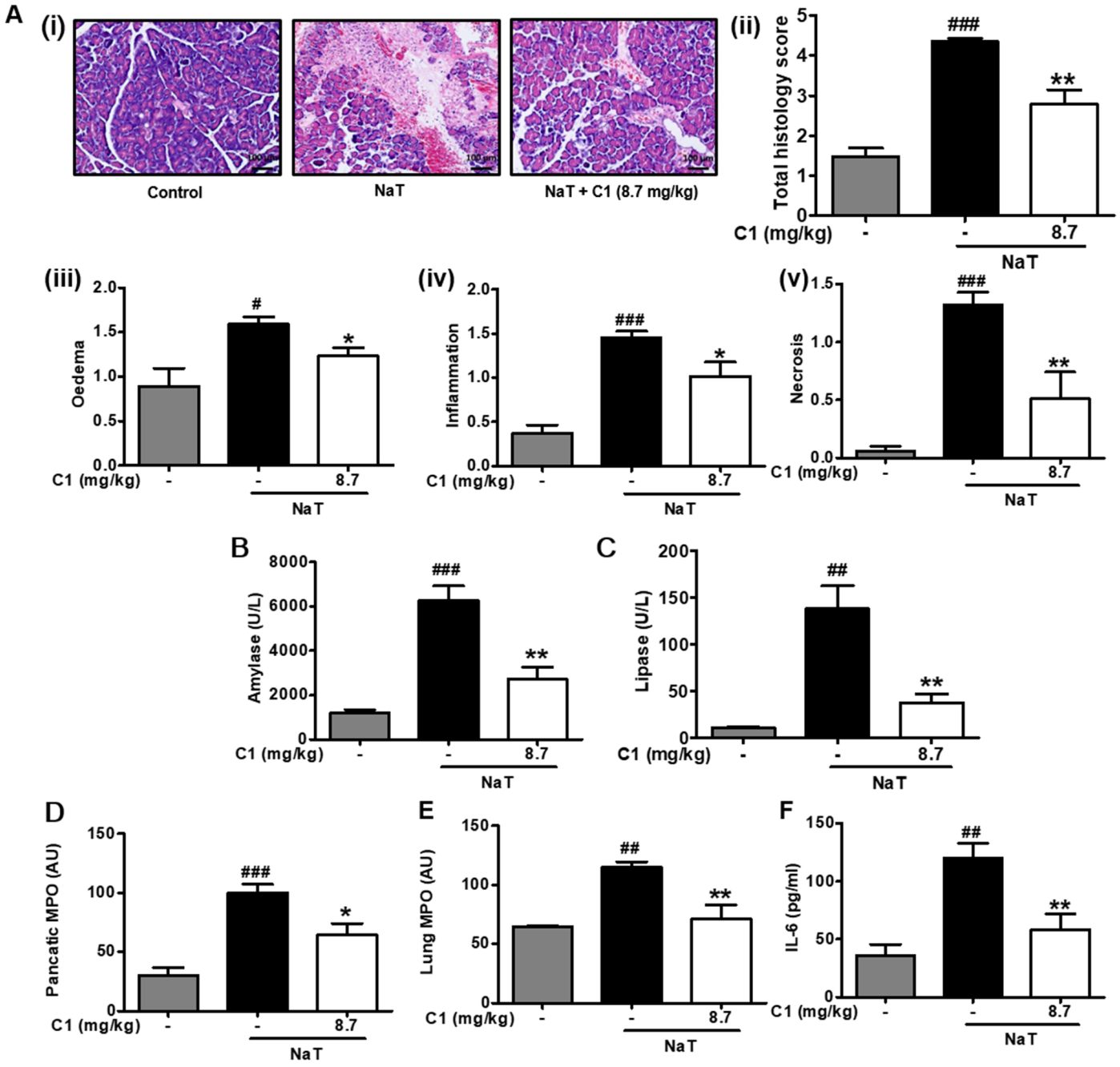
A
(i)
Control
NaT
NaT + C1 (8.7 mg/kg)
(ii)
Total histology score
###
**
C1 (mg/kg) - - 8.7
NaT
(iii)
Oedema
#
*
C1 (mg/kg) - - 8.7
NaT
(iv)
Inflammation
###
*
C1 (mg/kg) - - 8.7
NaT
(v)
Necrosis
###
**
C1 (mg/kg) - - 8.7
NaT
B
Amylase (U/L)
###
**
C1 (mg/kg) - - 8.7
NaT
C
Lipase (U/L)
##
**
C1 (mg/kg) - - 8.7
NaT
D
Pancatic MPO (AU)
###
*
C1 (mg/kg) - - 8.7
NaT
E
Lung MPO (AU)
##
**
C1 (mg/kg) - - 8.7
NaT
F
IL-6 (pg/ml)
##
**
C1 (mg/kg) - - 8.7
NaT

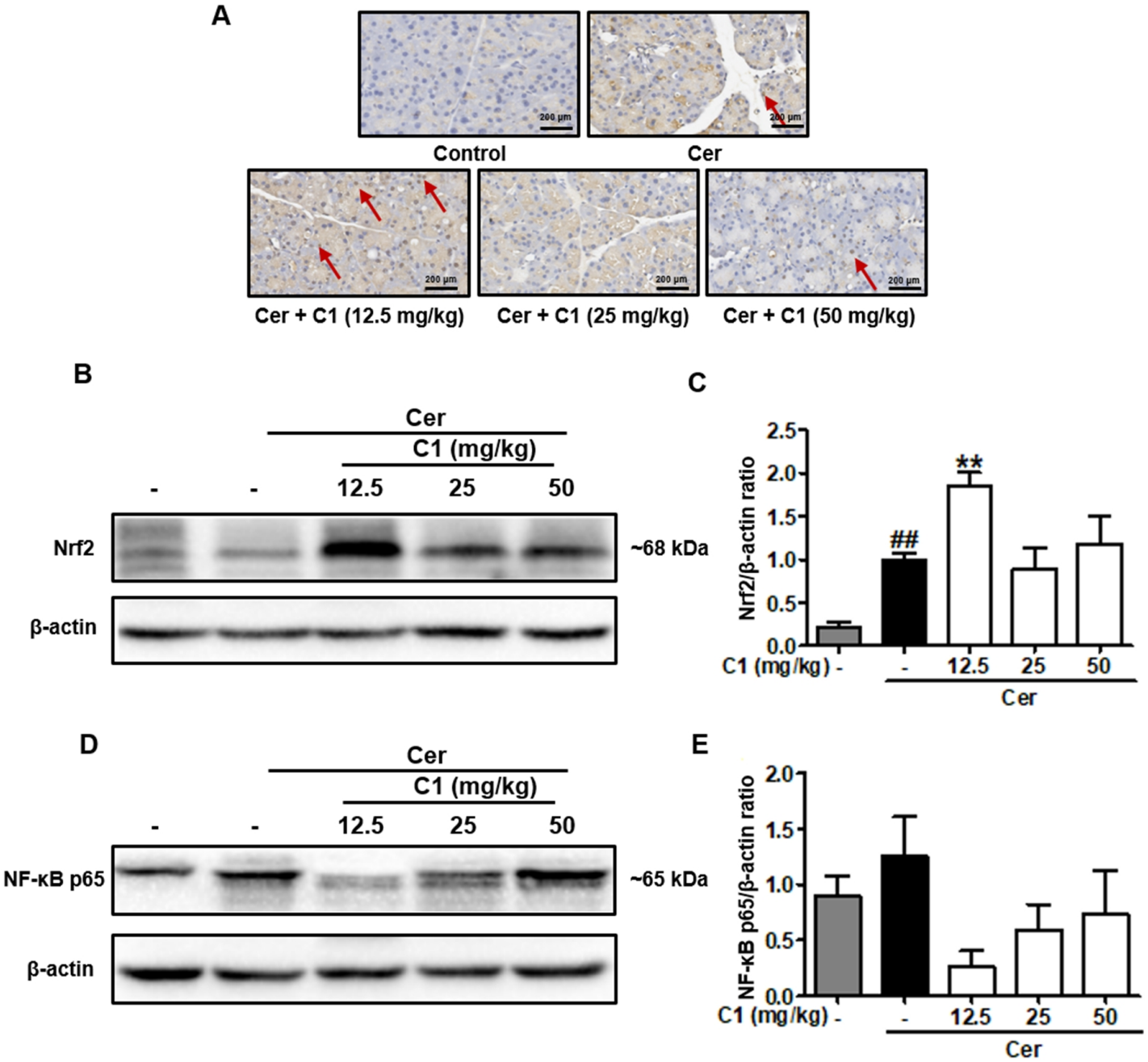
A
Control
Cer
Cer + C1 (12.5 mg/kg)
Cer + C1 (25 mg/kg)
Cer + C1 (50 mg/kg)
200 μm
B
Cer
C1 (mg/kg)
- - 12.5 25 50
Nrf2
β-actin
~68 kDa
C
Nrf2/β-actin ratio
2.5
2.0
1.5
1.0
0.5
0.0
##
**
C1 (mg/kg) - - 12.5 25 50
Cer
D
Cer
C1 (mg/kg)
- - 12.5 25 50
NF-κB p65
β-actin
~65 kDa
E
NF-κB p65/β-actin ratio
2.0
1.5
1.0
0.5
0.0
C1 (mg/kg) - - 12.5 25 50
Cer

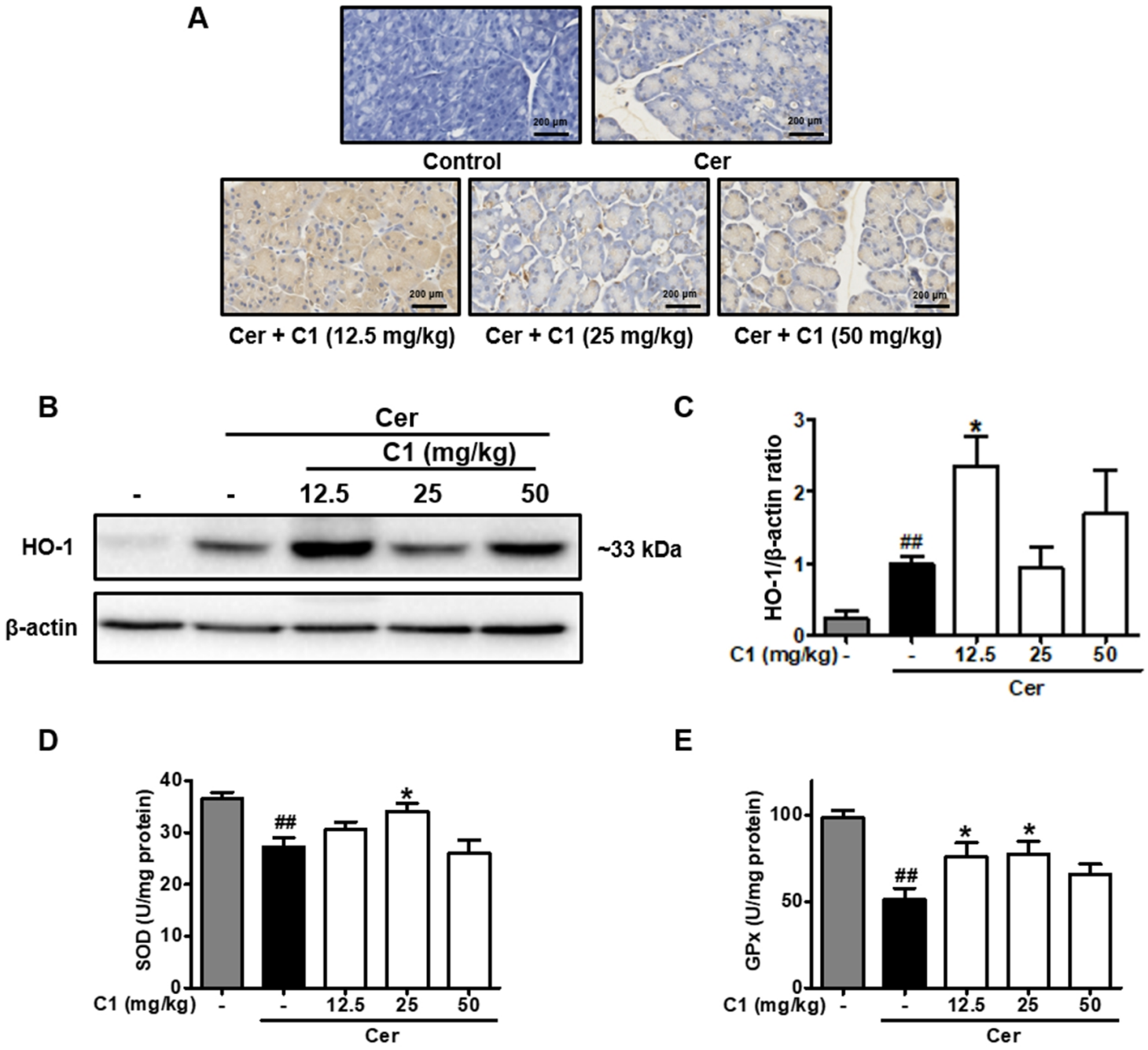
A
200 μm
Control
Cer
Cer + C1 (12.5 mg/kg)
Cer + C1 (25 mg/kg)
Cer + C1 (50 mg/kg)
B
Cer
C1 (mg/kg)
-
-
12.5
25
50
HO-1
~33 kDa
β-actin
C
HO-1/β-actin ratio
##
*
C1 (mg/kg)
Cer
D
SOD (U/mg protein)
E
GPx (U/mg protein)